thereby minimizing this interaction, but in solution the phenyl rings would normally rotate and this leads to even greater interaction. With use of the same bond distances for the *mer* isomer as those found for the *fac* isomer, molecular models show that this particular steric effect is completely absent in the *mer* isomer, but instead there is considerable strain in the formation of the two five-membered chelate rings, which originates in the unfavorable angles at the central phosphorus atom. The complexes are therefore subject to strain in both configurations and are not completely stable in either isomeric form for either the 18- or 17-electron configurations. For the present complexes in the 17-electron state these influences reveal themselves in both kinetic and thermodynamic effects, and they rapidly interconvert between the two highly strained isomeric structures. The effect of replacing three monodentate ligands with the tridentate P_2P' ligand is to increase the value of K_{fac^+/mer^+} by several orders of magnitude (Table I). However, the variation in K_{fac^+/mer^+} upon changing the metal is relatively small.

Acknowledgment. S.W.F. thanks the Deakin University Research Committee for the award of a Gordon Fellowship during a 1989 sabbatical leave. Support of the U.S. Department of Energy, under Contract No. DE-AC0276CH00016, is gratefully acknowledged. P.M. and T.W. thank the Australian Government for Postgraduate Research Awards. Funding provided by the Australian Research Council is also gratefully acknowledged.

Oxygen- and Carbon-Bound Ruthenium Enolates: Migratory Insertion, Reductive Elimination, β-Hydrogen Elimination, and Cyclometalation Reactions

John F. Hartwig, Robert G. Bergman,* and Richard A. Andersen*

Department of Chemistry, University of California, Berkeley, California 94720

Received March 26, 1991

The generation of a series of reactive ruthenium complexes of the general formula $(PMe_3)_4Ru(R)(enolate)$ is reported. Most of these enolates have been shown to bind to the ruthenium center through the oxygen atom. This binding mode is evident from solution NMR data as well as from an X-ray crystal structure of a representative example. Two of the enolate complexes **8** and **9** exist in equilibrium between the O- and C-bound forms; both isomers can be identified clearly by NMR spectroscopy. Variable-temperature NMR studies demonstrate that the ratio of the two isomers changes reversibly with temperature, demonstrating that it represents the equilibrium distribution. Synthesis of the bulky ruthenium enolate **10** results in dissociation of phosphine and formation of a complex in which the enolate hydrogen is coordinated to the metal center in an agostic binding mode. X-ray structural analysis demonstrates that the complex contains one Ru–O bond and one agostic interaction between the ruthenium center and the vinylic hydrogen. The reactions of these compounds include the β-migration of the phenyl group in $(PMe_3)_4Ru(Ph)(OC(CH_2)Me)$ (**4a**) to form oxametallacyclobutane $(PMe_3)_4Ru(OC(Me)(Ph)CH_2)$ (**11**). Heating $(PMe_3)_4Ru(H)(OC(CH_2)Me)$ with CO at 85 °C for 8 h led to reductive elimination of acetone and formation of the Ru(0) complex $(PMe_3)_2Ru(CO)_3$. Warming a solution of $(PMe_3)_4Ru(Me)(OC(CH_2)Me)$ to 65 °C led to β-hydrogen elimination, forming $(PMe_3)_4Ru(Me)(H)$. This transformation constitutes the formal elimination of ketene, and when this thermolysis was run in the presence of tert-butyl alcohol as a trap, *tert*-butyl acetate was formed in 10–15% yield, consistent with the formation of ketene during the course of the reaction. Addition of the potassium enolate of acetaldehyde to phenyl chloride $(PMe_3)_4Ru(Ph)(Cl)$ (**1**) yielded $(PMe_3)_3(CO)Ru(Ph)(Me)$. A mechanism initiated by an analogous β-hydrogen elimination reaction is proposed. Other enolate complexes undergo cyclometallation reactions to form oxygen-containing metallacycles. Thermolysis of $(PMe_3)_4Ru(Me)(OC(CH_2)Me)$ (a mixture of O- and C-bound isomers **8a** and **8b**) forms the acetone dianion complex $(PMe_3)_4Ru((CH_2)_2CO)$ (**14**). Cyclometalation of $(PMe_3)_4Ru(Me)(OC(CH_2)CMe_3)$ (**5c**) led to formation of the oxametallacyclobutene complex $(PMe_3)_4Ru(OC(CMe_3)CH)$ (**16**). Addition of 2 equiv of potassium enolate to $(PMe_3)_4Ru(OAc)(Cl)$ (**12**) also led to metallacyclic products. Reaction of 2 equiv of the potassium enolate of acetone with **12** yielded **14**, while 2 equiv of the potassium enolate of 4,4-dimethyl-2-pentanone provided oxametallacyclobutane $(PMe_3)_4Ru(OC(=CHCMe_3)CH_2)$ (**13**).

Introduction

Until recently, the organometallic chemistry of late-transition-metal systems has focused on metal–carbon and –hydrogen bonds. Many routes to formation of metal alkyl, aryl, allyl, and hydride complexes have been investigated, and reactions such as β-hydrogen elimination, reductive elimination, and migratory insertion are well documented. The preparation and reactivity of compounds containing late transition-metal–oxygen bonds is less common. It has been proposed that combining a hard ligand with a soft late-metal center may lead to weak late-metal–heteroatom linkages and result in reactive late-metal–heteroatom bonds.[1]

Several research groups have been interested in transition-metal–enolate complexes from the perspective of using the metal center as a potential site of asymmetry in the design of chiral catalysts for aldol reactions. Indeed, transition-metal-mediated aldol reactions have been observed,[2] and some systems undergo catalytic aldol reac-

(1) (a) Bryndza, H. E.; Tam, W. *Chem. Rev.* **1988**, *88*, 1163 and references therein. (b) Pearson, R. G. *J. Am. Chem. Soc.* **1963**, *85*, 3533.

(2) (a) Mukaiyama, T.; Banno, K.; Narasaka, K. *J. Am. Chem. Soc.* **1974**, *96*, 7503. (b) Evans, D. A.; McGee, L. R. *Tetrahedron Lett.* **1980**, 3975. (c) Yamamoto, Y.; Naruyama, K. *Tetrahedron Lett.* **1980**, 4607. (d) Stille, J. R.; Grubbs, R. H. *J. Am. Chem. Soc.* **1983**, *105*, 1665. (e) Sato, S.; Matsuda, I.; Izumi, Y. *Tetrahedron Lett.* **1986**, 5517. (f) Reetz, M. T.; Vougioukas, A. E. *Tetrahedron Lett.* **1987**, *28*, 793.

0276-7333/91/2310-3326$02.50/0

tions.[3] Transition-metal–enolate complexes also provide a unique system for comparing the structure and reactivity of late-metal–oxygen bonds to late-metal–carbon bonds. Enolates have been shown to bind to metal centers in an η^1-mode through the oxygen atom[4] or the methylene group[5] or in an η^3-mode as an oxaallyl.[6] Typically, early-transition-metal enolates exist in the O-bound form, while late-metal enolates are C-bound. Only a few cases of late-transition-metal O-bound enolates are known.[3,4j,k]

During the course of our studies with the L_4Ru metal system (L = PMe_3) we discovered the propensity of enolate substituents to bind to the ruthenium center through the oxygen atom rather than the methylene.[7] Initial studies indicated that this unusual bonding mode gives rise to unprecedented reactivity, and we decided to investigate the synthesis and reactivity of a series of O-bound ruthenium enolates. We provide here a general method for the preparation of a series of O-bound ruthenium enolates and report their rich reactivity, which includes processes such as reductive elimination, β-phenyl migration, β-hydrogen elimination, and cyclometalation to form oxametallacycles. Studies of the structure and reactivity of the resulting metallacycles is reported in a companion paper.[8]

Results

Synthesis of O-Bound Enolates. The general synthesis of the ruthenium enolate complexes is shown in eq 1. Addition of the potassium enolates of a variety of ketones and aldehydes at room temperature to ruthenium hydrido, alkyl, and aryl halide complexes led in most cases to the generation of O-bound enolates. Exceptions are the addition of the potassium enolate of acetone and 4,4-dimethyl-2-pentanone (methyl neopentyl ketone) to $(PMe_3)_4Ru(Me)(Cl)$, which provided equilibrium mixtures of both the O- and C-bound forms of enolates 8 and 9 (eq 2). The potassium counterion was important for these substitution reactions. Addition of the lithium enolate of acetone to the ruthenium phenyl chloride (1) led to no reaction, even in THF solvent or with the addition of the appropriate crown ether. The potassium enolates were isolated as solids in the drybox, and they were stored for up to a week in a −40 °C freezer.

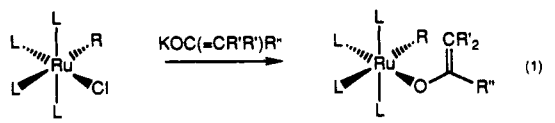

1 R=Ph
2 R=Me
3 R=H

4a R=Ph, R'=H, R"=Me
5a R=Me, R'=Me, R"=H
5b R=Me, R'=H, R"=H
5c R=Me, R'=H, R"=*tert*-Bu
6a R=H, R'=H, R"=Me

Scheme I

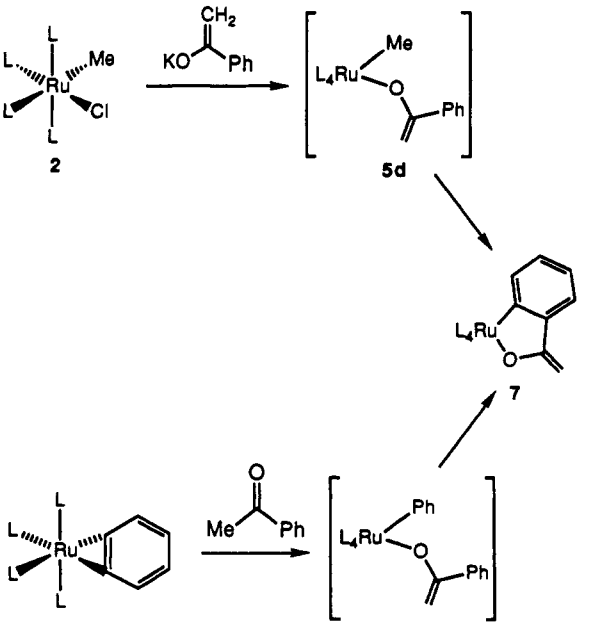

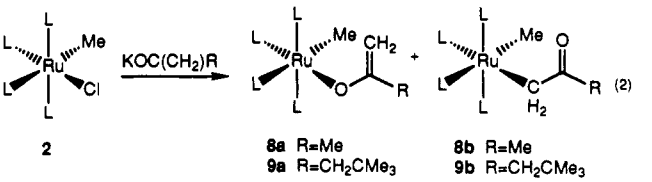

2

8a R=Me
9a R=CH_2CMe_3

8b R=Me
9b R=CH_2CMe_3

The compounds $(PMe_3)_4Ru(Me)(OC(CMe_2)Me)$ (**5a**) and $(PMe_3)_4Ru(H)(OC(CH_2)Me)$ (**6a**) were isolated in pure form and were characterized by microanalysis, as well as ^1H, $^{31}P\{^1H\}$, and $^{13}C\{^1H\}$ NMR and infrared spectroscopy. The orthometalated enolate **7** was prepared by addition of the potassium enolate of acetophenone to methyl chloride **2**[9] as shown in Scheme I or by addition of acetophenone to the benzyne complex $(PMe_3)_4Ru(\eta^2\text{-}C_6H_4)$.[10] This enolate was characterized by X-ray diffraction, as well as microanalysis, ^1H, $^{31}P\{^1H\}$, and $^{13}C\{^1H\}$ NMR, and infrared spectroscopy. The other O-bound ruthenium enolates in this study were not stable enough at room temperature to isolate, and so these were characterized by solution NMR spectroscopy.

NMR spectroscopic data for the compounds prepared in this study are included in Tables VI–VIII. The ^1H NMR spectrum of all the O-bound enolates contained two inequivalent resonances between δ 3.4 and 4.2 for the olefinic hydrogens. In addition, the $^{13}C\{^1H\}$ NMR spectra contained CH_2 resonances (confirmed by DEPT pulse sequence) between δ 73 and 94. The $^{31}P\{^1H\}$ spectra of the hydrido, alkyl, and aryl ruthenium enolates all displayed

(3) Slough, G. A.; Bergman, R. G.; Heathcock, C. H. *J. Am. Chem. Soc.* **1989**, *111*, 938.

(4) Zirconium: (a) Manriquez, J. M.; McAlister, D. R.; Sanner, R. D.; Bercaw, J. E. *J. Am. Chem. Soc.* **1978**, 2716. (b) Gambarotta, S.; Florianai, C.; Chiesi,-Villa, A.; Guastini, C. *J. Am. Chem. Soc.* **1983**, *105*, 1690. (c) Moore, E. J.; Straus, D. A.; Armantrout, J.; Santarsiero, B. D.; Grubbs, R. H.; Bercaw, J. E. *J. Am. Chem. Soc.* **1983**, *105*, 2068. Titanium: (d) Curtis, D. M.; Thanedar, S.; Butler, W. M. *Organometallics* **1984**, *3*, 1855. (e) Straus, D. A.; Grubbs, R. H. *J. Am. Chem. Soc.* **1982**, *104*, 5499. (f) Fachinetti, G.; Biran, C.; Florianai, C.; Villa, A. C.; Buastini, C. *Inorg. Chem.* **1978**, *17*, 2995. Thorium: (g) Fagan, P. J.; Manriquez, J. M.; Marks, T. J.; Day, V. W.; Vollmer, S. H.; Day, C. S. *J. Am. Chem. Soc.* **1980**, *102*, 5393. (h) Sonnenberger, D. C.; Mintz, E. A.; Marks, T. J. *J. Am. Chem. Soc.* **1984**, *106*, 3484. Molybdenum: (i) Hirao, T.; Fujihara, Y.; Tsuno, S.; Ohshiro, Y.; Agawa, T. *Chem. Lett.* **1984**, 367. Palladium: (j) Ito, Y.; Nakatsuka, M.; Kise, N.; Saegusa, T. *Tetrahedron Lett.* **1980**, *21*, 2873. (k) Dall'Antonia, P.; Graziani, M.; Lenarda, M. *J. Organomet. Chem.* **1980**, *186*, 131.

(5) Burkhardt, E. R.; Doney, J. J.; Bergman, R. G.; Heathcock, C. H. *J. Am. Chem. Soc.* **1987**, *109*, 2022. An extensive list of C-bound enolates is provided in this paper.

(6) (a) Guggolz, E.; Ziegler, M.; Biersack, H.; Herrmann, W. A. *J. Organomet. Chem.* **1980**, *194*, 317. (b) Bennett, M. A.; Robertson, G. B.; Watt, T.; Whimp, P. O. *J. Chem. Soc., Chem. Commun.* **1971**, 752. (c) Ito, Y.; Aoyama, H.; Hirao, T.; Mochizuki, A.; Saegusa, T. *J. Am. Chem. Soc.* **1979**, *101*, 494. (d) Holmgren, J. S.; Shapley, J. R.; Wilson, S. R.; Pennington, W. T. *J. Am. Chem. Soc.* **1986**, *108*, 508. (e) Robertson, G. B.; Whimp, P. O. *Inorg. Chem.* **1973**, *12*, 1740.

(7) (a) Hartwig, J. F.; Bergman, R. G.; Andersen, R. A. *J. Am. Chem. Soc.* **1990**, *112*, 3234. (b) Hartwig, J. F.; Bergman, R. G.; Andersen, R. A. *J. Am. Chem. Soc.* **1990**, *112*, 5670.

(8) Hartwig, J. F.; Bergman, R. G.; Andersen, R. A. *Organometallics*, following paper in this issue.

(9) Statler, J. A.; Wilkinson, G.; Thornton-Pett, M.; Hursthouse, M. B. *J. Chem. Soc., Dalton Trans.* **1984**, 1731.

(10) Hartwig, J. F.; Bergman, R. G.; Andersen, R. A. *J. Am. Chem. Soc.* **1989**, *111*, 2717; **1991**, *113*, 3404.

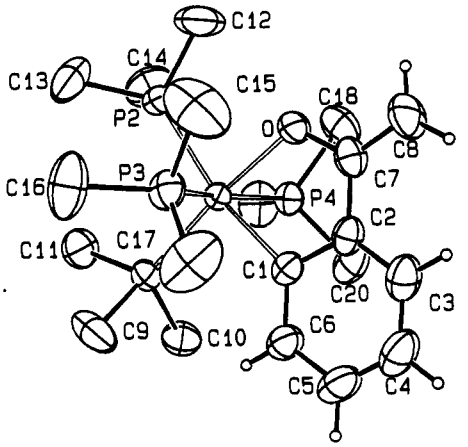

Figure 1. ORTEP drawing of 7. The hydrogen atoms of the PMe_3 ligands have been removed for clarity.

A_2BC $^{31}P\{^1H\}$ NMR spectra with P_B resonating downfield and P_C resonating upfield of P_A. The $^{31}P\{^1H\}$ NMR chemical shift of each ligand reflects the trans influence of the ligand located trans to it.[11] For example, the chemical shifts for the phosphines trans to alkoxide,[12] amide,[10,13] halide, and psuedohalides[8,14] in this metal–ligand system lie substantially downfield from those of the mutually trans phosphines, and the chemical shifts of the phosphines trans to hydride,[9,15] alkyl,[9,15] and aryl[15,16] substituents lie upfield of the mutually trans phosphines. Therefore $^{31}P\{^1H\}$ NMR spectroscopy is a useful indicator of the O- or C-bound form of these ruthenium enolates.

The solid-state structure of 7 confirmed the assignments of these O-bound enolates by solution NMR spectroscopy, and it provides the first X-ray structural information on a late-metal O-bound enolate. Compound 7 crystallized in space group $P\bar{1}$ with no abnormally short intermolecular contacts. An ORTEP drawing of the molecule is shown in Figure 1; crystal and data collection parameters are included in Table I and intramolecular distances and angles are provided in Tables II and III. The ruthenium atom in this complex is coordinated in an approximately octahedral fashion. The Ru–O distance is 2.120 (1) Å, similar to a Ru–O distance in a monomeric cresolate complex (2.161 (4) Å) and a monomeric phenyl hydroxide complex (2.145 (4) Å) of this metal–ligand system.[12,13] The Ru–C bond length (2.100 (1) Å) is similar to that observed in the analogous orthometalated benzyl (2.118 (3) Å)[17] and benzyne complexes (2.072 (2), 2.111 (2) Å).[9] The η^1-aryl distance of $(PMe_3)_4Ru(Ph)(OH)$ (2.159 (5) Å)[12] is slightly longer than those in the metallacycles. The surface defined by the organic ligand, P1, and P2 is planar to ±0.06 Å. Detailed analysis of the ligand geometry, however, shows that there is a slight twist (3.0 (9)°) of the $CC(O)CH_2$ group around the C2–C7 bond. The two axial Ru–P bonds are the same length, but the Ru–P (trans to oxygen) distance is significantly shorter than the other three Ru–P distances, reflecting the usual trans influence series in these molecules and in others.[10]

The identity of the oxygen and CH_2 groups was based on the unequivocal location of the two hydrogens on C8 in the difference Fourier map and is consistent with solution NMR data. The bond distances C7–O and C7–C8 indicate that some delocalization may be occurring. However, the distances in the phenyl group are most likely due to systematic effects of thermal motion, rather than to any peculiar electronic effects.

Synthesis of O- and C-Bound Enolates in Equilibrium. Two enolate complexes were obtained as an equilibrium mixture of their O- and C-bound forms. The addition of the potassium enolate of acetone to $(PMe_3)_4Ru(Me)(Cl)$[8] (2) in aromatic or ethereal solvents led to **8a,b** (eq 2). These two compounds were always

Table I. Crystal and Data Collection Parameters[a]

	7	10
temp, °C	25	−90
empirical formula	$RuP_4OC_{20}H_{42}$	$RuP_3OC_{25}H_{49}$
fw	523.5	559.7
cryst size, mm	0.25 × 0.28 × 0.30	0.25 × 0.30 × 0.50
space group	$P\bar{1}$	$P2_1/n$
a, Å	9.3452 (9)	8.918 (2)
b, Å	9.7161 (9)	37.441 (9)
c, Å	16.278 (2)	9.304 (9)
α, deg	97.511 (10)	90.0
β, deg	117.000 (8)	110.71 (2)
γ, deg	90.576	90.0
V, Å^3	2301.5 (6)	2905.7 (26)
Z	2	4
d_{calc}, g cm^{-3}	1.34	1.43
μ_{calc}, cm^{-1}	8.4	7.1
rflns measured	$+h, \pm k, \pm l$	$+h, +k, \pm l$
scan width	$\Delta\theta = 0.55 + 0.35 \tan\theta$	$\Delta\theta = 0.60 + 0.35 \tan\theta$
scan speed (θ, deg/min)	6.70	6.70
setting angles (2θ, deg)[b]	26–30	22–26

[a] Parameters common to both structures: radiation, Mo Kα; monochromator, highly oriented graphite (2θ = 12.2°); detector, crystal scintillation counter, with PHA; scan type, θ–2θ; background, measured over 0.25($\Delta\theta$) added to each end of the scan; vertical aperture = 3.0 mm; horizontal aperture = 2.0 + 1.0 tan θ mm; intensity standards, measured every hour of X-ray exposure time; orientation, three reflections were checked after every 200 measurements; crystal orientation was redetermined if any of the reflections were offset from their predicted positions by more than 0.1°. [b] Unit cell parameters and their esd's were derived by a least-squares fit to the setting angles of the unresolved Mo Kα components of 24 reflections with the given 2θ range. In this and all subsequent tables the esd's of all parameters are given in parentheses, right-justified to the least significant digit(s) of the reported value.

Table II. Intramolecular Distances for 7

atom 1	atom 2	dist, Å	atom 1	atom 2	dist, Å
Ru	P1	2.275 (1)	C5	C6	1.391 (2)
Ru	P2	2.375 (1)	P1	C9	1.843 (2)
Ru	P3	2.357 (1)	P1	C10	1.836 (2)
Ru	P4	2.357 (1)	P1	C11	1.839 (2)
Ru	O	2.120 (1)	P2	C12	1.813 (2)
Ru	C1	2.100 (1)	P2	C13	1.838 (2)
C7	C8	1.351 (2)	P2	C14	1.835 (2)
C7	O	1.331 (2)	P3	C15	1.820 (2)
C2	C7	1.478 (2)	P3	C16	1.822 (2)
C1	C2	1.419 (2)	P3	C17	1.811 (2)
C1	C6	1.400 (2)	P4	C18	1.829 (2)
C2	C3	1.392 (2)	P4	C19	1.835 (2)
C3	C4	1.376 (3)	P4	C20	1.823 (2)
C4	C5	1.368 (3)			

(11) A trans influence series is given in: Appleton, T. G.; Clark, H. C.; Manger, L. E. *Coord. Chem. Rev.* **1973**, *10*, 335. Discussion of correlations between trans influence and ^{31}P chemical shifts is found in: (a) Nixon, G. F.; Pidcock, A. *Annu. Rev. NMR Spectrosc.* **1969**, *2*, 345. (b) Verkade, J. M., Quin, Eds. *Phosphorus-31 NMR Spectroscopy in Stereochemical Analysis*; VCH Publishers: New York, 1987. (c) Meek, D. W.; Mazanec, T. J. *Acc. Chem. Res.* **1981**, *14*, 266.

(12) Hartwig, J. F.; Bergman, R. G.; Andersen, R. A. *J. Organomet. Chem.* **1990**, *394*, 417.

(13) Hartwig, J. F.; Andersen, R. A.; Bergman, R. G. *Organometallics* **1991**, *10*, 1875.

(14) Mainz, V. V.; Andersen, R. A. *Organometallics* **1984**, *3*, 675.

(15) Hartwig, J. F.; Andersen, R. A.; Bergman, R. G. *J. Am. Chem. Soc.*, in press.

(16) Jones, R. A.; Wilkinson, G. *J. Chem. Soc., Dalton Trans.* **1979**, 472.

(17) Tulip, T. H., personal communication.

Table III. Intramolecular Angles for 7

atom 1	atom 2	atom 3	angle, deg
P1	Ru	P2	97.17 (1)
P1	Ru	P3	97.38 (2)
P1	Ru	P4	94.71 (1)
P2	Ru	P3	93.81 (2)
P2	Ru	P4	93.83 (1)
P3	Ru	P4	164.77 (2)
P1	Ru	O	174.59 (3)
P2	Ru	O	88.09 (3)
P3	Ru	O	83.47 (3)
P4	Ru	O	83.64 (3)
P1	Ru	C1	95.80 (4)
P2	Ru	C1	167.03 (4)
P3	Ru	C1	84.30 (4)
P4	Ru	C1	85.30 (4)
O	Ru	C1	78.95 (5)
Ru	C1	C2	112.88 (11)
Ru	C1	C6	130.91 (12)
Ru	O	C7	116.16 (9)
C2	C1	C6	116.20 (14)
C1	C2	C3	120.76 (16)
C1	C2	C7	116.48 (13)
C3	C2	C7	122.76 (15)
C2	C3	C4	120.93 (17)
C3	C4	C5	119.68 (16)
C4	C5	C6	120.23 (17)
C1	C6	C5	122.19 (17)
C2	C7	C8	123.94 (16)
C2	C7	O	115.39 (13)
O	C7	C8	120.67 (16)
Ru	P1	C9	117.90 (7)
Ru	P1	C10	118.91 (6)
Ru	P1	C11	120.26 (7)
C9	P1	C10	98.97 (9)
C9	P1	C11	98.84 (10)
C10	P1	C11	97.54 (9)
Ru	P2	C12	111.78 (7)
Ru	P2	C13	121.93 (8)
Ru	P2	C14	123.21 (7)
C12	P2	C13	99.38 (12)
C12	P2	C14	99.11 (11)
C13	P2	C14	96.83 (11)
Ru	P3	C15	112.77 (8)
Ru	P3	C16	124.72 (8)
Ru	P3	C17	118.47 (7)
C15	P3	C16	99.42 (13)
C15	P3	C17	98.50 (14)
C16	P3	C17	98.44 (12)
Ru	P4	C18	113.20 (6)
Ru	P4	C19	122.86 (7)
Ru	P4	C20	117.65 (6)
C18	P4	C19	99.98 (9)
C18	P4	C20	100.29 (9)
C19	P4	C20	99.18 (9)

observed in the same 3:1 ratio in C_6D_6 solvent at room temperature, suggesting that this is the equilibrium mixture. Indeed, the two isomers were shown to rapidly interconvert on the laboratory time scale (vide infra). Therefore, they were characterized as a 3:1 mixture by solution NMR and infrared spectroscopy, as well as microanalysis. The O-bound isomer **8a** displayed spectroscopic features analogous to those of the other O-bound enolates. Resonances for three phosphine methyl groups in a ratio of 2:1:1 were observed in the ^1H NMR spectrum, along with two olefinic hydrogens at δ 3.50 and 3.96 and an enolate methyl group at δ 2.06. A metal-bound methyl group resonated at δ 0.40.

The C-bound isomer **8b** exhibited three phosphine methyl groups in a 2:1:1 ratio and an enolate methyl group at δ 2.00, along with a second metal-bound methyl group at δ −0.26. The $^{13}C\{^1H\}$ NMR spectrum indicated the presence of a Ru–C bond in this compound. A CH_2 resonance in the $^{13}C\{^1H\}$ NMR spectrum was observed at δ 22.83, clearly out of the range of methylene resonances for

Scheme II

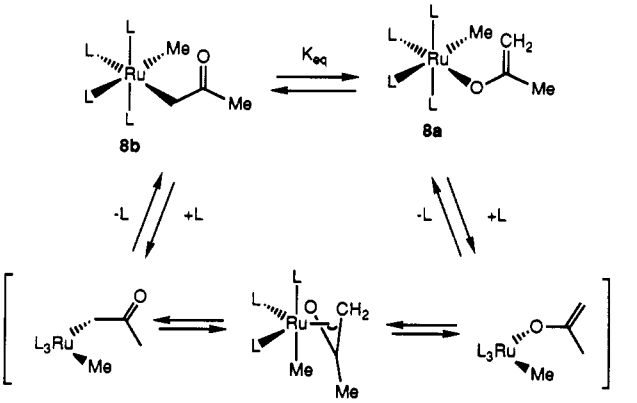

O-bound enolates. In addition, the resonance appeared as a multiplet that displayed coupling to several phosphorus atoms, indicating that this carbon atom is bound to the ruthenium center. The $^{31}P\{^1H\}$ NMR spectrum was also consistent with a mixture of O- and C-bound enolates. In addition to the typical $^{31}P\{^1H\}$ NMR spectrum for the O-bound enolate complexes, the $^{31}P\{^1H\}$ NMR spectrum of this mixture displayed an A_2BC pattern in which both P_B and P_C resonated significantly upfield of the phosphines located trans to O-bound enolates in this system. The chemical shift of these phosphines was closer to the region of PMe_3 ligands trans to simple L_4Ru alkyls.

Addition of the *tert*-butyl-substituted analogue $KOC(CH_2)CH_2CMe_3$ to $(PMe_3)_4Ru(Me)(Cl)$ (**2**) also led to formation of a mixture of O- and C-bound ruthenium enolates **9a** and **9b**. Two neopentyl groups were observed in the ^1H and $^{13}C\{^1H\}$ NMR spectra, as well as two metal-bound methyl groups. The methylene resonances of the O-bound form were observed at δ 3.05 and 3.78 in the ^1H NMR spectrum and at δ 79.45 in the $^{13}C\{^1H\}$ NMR spectrum. The CH_2 portion of the C-bound enolate resonated as a multiplet at δ 1.96 in the ^1H NMR spectrum and as a doublet of multiplets (J_{PC} = 42.2 Hz) in the $^{13}C\{^1H\}$ NMR spectrum. The two patterns in the $^{31}P\{^1H\}$ NMR spectrum were nearly identical with those of the acetone enolates **8a** and **8b**.

In order to demonstrate that the ratio of these isomers resulted from rapid equilibration, it was necessary to obtain mixtures containing enhanced amounts of each isomer and then show that these both return to the equilibrium ratio. To do this in a simple way, a solution of these isomers was monitored by ^1H and $^{31}P\{^1H\}$ NMR spectroscopy at different temperatures. At 5 °C the observed ratio of **8a** to **8b** by ^1H NMR spectroscopy was 2.78, and at 60 °C it was 4.46. Both of these mixtures returned rapidly to a 3.50 ratio at 25 °C. At 5 °C equilibrium was established over the course of 10–15 min; nonequilibrium ratios were never observed above 40 °C, indicating that interconversion occurs rapidly on the laboratory time scale at these temperatures.

A plot of ln K versus $1/T$ for the equilibrium written in Scheme II is displayed in Figure 2 and indicates that ΔH (1.5 ± 0.2 kcal/mol) favors the C-bound form and ΔS (7.6 ± 2.0) favors the O-bound form. The values for both of these parameters are small but significantly different from zero. The equilibrium ratios were reproducible to within 5–10%, and the slope of the ln K versus $1/T$ plot for the equilibrium indicated in Scheme II is clearly negative. Since the dominant form of this complex at room temperature is O-bound, the value of ΔS must be positive, although the absolute value is small. We did not perform this experiment with the *tert*-butyl-substituted analogue

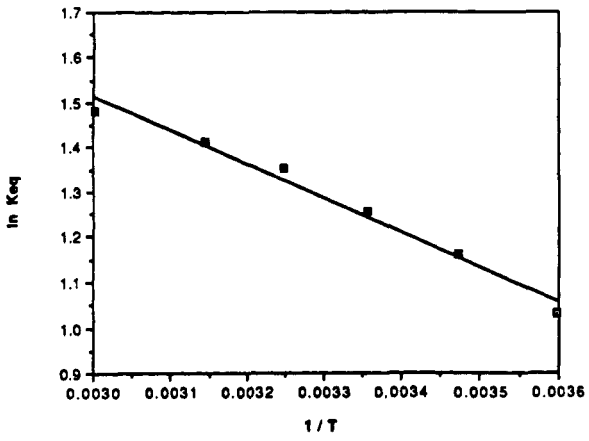

Figure 2. Plot of ln K versus $1/T$ to obtain thermodynamic parameters for the equilibrium shown in Scheme II.

Scheme III

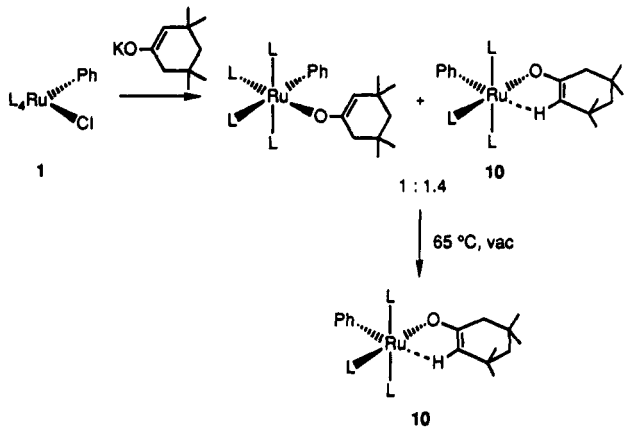

9, but we presume that the ratio of isomers observed with this compound at room temperature is also a result of facile equilibration.

A qualitative comparison of the rates of phosphine dissociation and approach to equilibrium was performed by adding 4 equiv of PMe_3-d_9 to a sample of the two isomers and monitoring the solution at 0 °C by $^{31}P\{^1H\}$ NMR spectroscopy. Over the course of 5–10 min, complete exchange of the free, labeled phosphine and unlabeled, coordinated phosphine was observed, as determined by observing a 1:1 ratio of free PMe_3-d_9 and free PMe_3-d_0. Thus, the rate of phosphine dissociation is faster than the interconversion of **8a** and **8b**.

Synthesis of an Enolate Complex with an Agostic Vinyl Hydrogen. A complex containing an oxaallyl (η^3-bound enolate) ligand is a possible intermediate in this exchange process. We set out to isolate an η^3-enolate bound to the $L_3Ru(R)$ metal center by using a large enolate substituent, which would favor dissociation of phosphine. Indeed, addition of the potassium enolate of 3,3,5,5-tetramethylcyclohexanone to the phenyl chloride **1** led to formation of a 1:1.4 ratio of a compound containing four phosphines, to which we assign the simple O-bound structure shown in Scheme III, and compound **10**, containing three phosphines. The $^{31}P\{^1H\}$ NMR spectrum of the L_4Ru complex was consistent with those of the other η^1-O-bound enolate complexes. Removal of toluene solvent under vacuum at 65 °C led to complete conversion to **10**. This material possesses two mutually trans phosphines and one resonating in the region characteristic of phosphines located trans to other oxygen-containing substituents. However, several spectroscopic characteristics are consistent with an η^3-binding mode. First, only two enolate

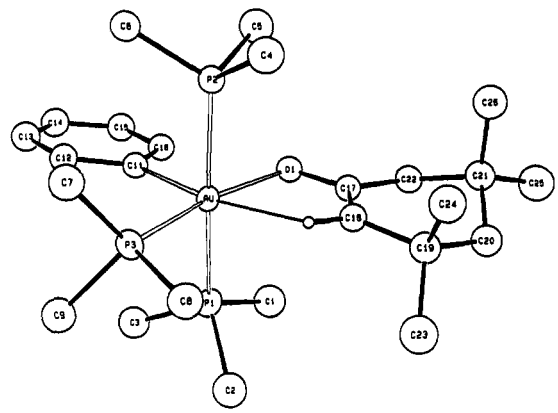

Figure 3. ORTEP drawing of **10**. The position of the vinylic hydrogen atom in the drawing is based on indealized sp^2 geometry.

Table IV. Intramolecular Distances for 10

atom 1	atom 2	dist, Å	atom 1	atom 2	dist, Å
Ru	P1	2.349 (1)	C21	C25	1.560 (6)
Ru	P2	2.332 (1)	C21	C26	1.539 (6)
Ru	P3	2.251 (1)	C11	C12	1.415 (6)
Ru	O1	2.127 (3)	C11	C16	1.423 (6)
Ru	C11	2.030 (4)	C12	C13	1.408 (6)
Ru	C17	2.776 (4)	C13	C14	1.364 (6)
Ru	C18	2.766 (4)	C14	C15	1.413 (6)
Ru	H18	2.14	C15	C16	1.403 (6)
O1	C17	1.314 (4)	P1	C1	1.855 (5)
C17	C18	1.352 (5)	P1	C2	1.862 (5)
C17	C22	1.526 (5)	P1	C3	1.844 (5)
C18	C19	1.534 (5)	P2	C4	1.849 (5)
C19	C20	1.562 (6)	P2	C5	1.824 (5)
C19	C23	1.553 (6)	P2	C6	1.834 (4)
C19	C24	1.549 (6)	P3	C7	1.856 (4)
C20	C21	1.550 (6)	P3	C8	1.855 (4)
C21	C22	1.556 (6)	P3	C9	1.848 (4)

methyl groups and two methylenes were observed in the ^1H NMR spectrum, indicating that the two sides of the six-membered ring are chemically equivalent. Either interconversion between binding to the two sides of the η^3-bound enolate occurs rapidly on the NMR time scale or the ligand is bound in a more symmetrical fashion. Second, the CH group of the enolate was observed at δ −1.25 in the ^1H NMR spectrum, far from the chemical shift region usual for vinylic hydrogens. However, the $^{13}C\{^1H\}$ NMR chemical shift of the methine carbon was δ 76.97, similar to the vinylic resonances of the other enolates reported above.

A single crystal suitable for an X-ray diffraction study was obtained by slow evaporation of a pentane solution of **10**. The structure was solved by standard Patterson and least-squares techniques. An ORTEP drawing of the molecule is shown in Figure 3. Crystal and data collection parameters are included in Table I; intramolecular distances and angles are provided in Tables IV and V. Consistent with the solution NMR data, the enolate is bound symmetrically, and an apparent agostic interaction exists between the metal center and the vinylic C–H bond. The hydrogen atom was not located or refined. Its assumed position is based on idealized sp^2 geometry, but the existence of an agostic interaction is consistent with the ^1H and $^{13}C\{^1H\}$ NMR chemical shifts, indicating that this binding mode exists in solution as well as in the solid state. The overall geometry is pseudooctahedral with the agostic C–H bond occupying one coordination site. As deduced from the $^{31}P\{^1H\}$ NMR spectrum, two phosphines are bound trans to each other and the other is located trans to the oxygen atom of the enolate. The ring is distorted

Table V. Intramolecular Angles for 10

atom 1	atom 2	atom 3	angle, deg	atom 1	atom 2	atom 3	angle, deg
P1	Ru	P2	170.66 (4)	Ru	P1	C1	113.55 (15)
P1	Ru	P3	93.07 (4	Ru	P1	C2	119.70 (15)
P1	Ru	O1	86.59 (7)	Ru	P1	C3	117.46 (15)
P1	Ru	C11	88.47 (11)	C1	P1	C2	100.41 (21)
P2	Ru	P3	95.54 (4)	C1	P1	C3	100.81 (20)
P2	Ru	O1	85.77 (7)	C2	P1	C3	101.95 (21)
P2	Ru	C11	86.71 (11)	Ru	P2	C4	117.65 (15)
P3	Ru	O1	167.78 (7)	Ru	P2	C5	111.68 (15)
P3	Ru	C11	98.27 (11)	Ru	P2	C6	120.53 (14)
O1	Ru	C11	93.93 (13)	C4	P2	C5	101.49 (21)
Ru	O1	C17	105.08 (22)	C4	P2	C6	102.49 (20)
O1	C17	C18	123.1 (4)	C5	P2	C6	100.05 (20)
O1	C17	C22	114.6 (3)	Ru	P3	C7	123.97 (15)
C18	C17	C22	122.3 (4)	Ru	P3	C8	109.74 (14)
C17	C18	C19	125.9 (4)	Ru	P3	C9	122.23 (15)
C18	C19	C20	109.6 (3)	C7	P3	C8	98.04 (20)
C18	C19	C23	110.6 (3)	C7	P3	C9	97.80 (20)
C18	C19	C24	110.5 (3)	C8	P3	C9	100.39 (20)
C20	C19	C23	106.4 (3)				
C20	C19	C24	112.1 (3)				
C23	C19	C24	107.4 (4)				
C19	C20	C21	116.2 (3)				
C20	C21	C22	108.3 (3)				
C20	C21	C25	108.8 (3)				
C20	C21	C26	113.5 (3)				
C22	C21	C25	108.5 (3)				
C22	C21	C26	109.8 (3)				
C25	C21	C26	107.8 (3)				
C17	C22	C21	112.0 (3)				
Ru	C11	C12	128.0 (3)				
Ru	C11	C16	116.0 (3)				
C12	C11	C16	116.0 (4)				
C11	C12	C13	122.1 (4)				
C12	C13	C14	121.1 (4)				
C13	C14	C15	118.9 (4)				
C14	C15	C16	120.7 (4)				
C11	C16	C15	121.3 (4)				

from planarity, as is expected for a six-membered ring system; rapid inversion accounts for the equivalence of C23 and C24 as well as C25 and C26 in the ^1H and $^{13}C\{^1H\}$ NMR spectrum. The Ru–O distance (2.127 (3) Å) is similar to the Ru–O distance (2.120 (1) Å) in the orthometalated enolate 7. The Ru–C17 and Ru–C18 distances of 2.776 (4) and 2.776 (4) Å indicate that the olefinic portion of the enolate is not directly bonded to the metal center. Consistent with an uncoordinated C–C double bond, the C17–C18 distance is not unusually long (1.352 (5) Å) and is similar to the uncoordinated C–C double bond distance of 1.351 (2) Å in 7.

Synthesis of Metallacycles. The addition of the potassium enolate of acetone to phenyl chloride 1 at room temperature led to formation of the oxametallacylobutane complex[7a] $(PMe_3)_4Ru(OC(Me)(Ph)CH_2)$ (**11a**), as determined by ^1H, $^{13}C\{^1H\}$, and $^{31}P\{^1H\}$ NMR spectroscopy at −40 °C (eq 3). The room temperature ^1H NMR spectrum

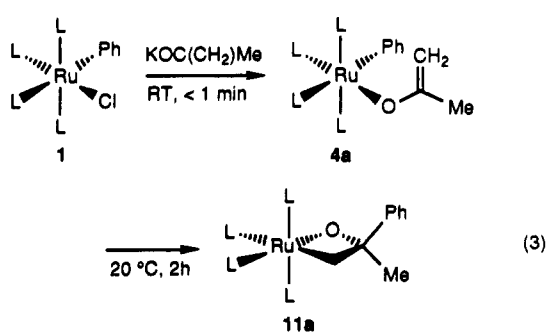

(3)

of this material displayed broad resonances and the room temperature $^{31}P\{^1H\}$ NMR spectrum contained no observable resonances. We presume that rapid, reversible dissociation of phosphine is responsible for the spectroscopic changes between room temperature and −40 °C. Removal of solvent led to decomposition of the ruthenium complex, thus preventing isolation of this material in pure form.

However, an isolable analogue of **11a** was obtained by the addition of 2 equiv of DMPE (1,2-*bis*(dimethylphosphino)ethane) to a benzene solution of **11a**, and this confirms the structural assignment of the PMe_3 complex. This simple ligand substitution product $(DMPE)_2Ru(OC(Me)(Ph)CH_2)$ (**11b**) was isolated after a reaction time of 2 h at room temperature (eq 4). The chelating phosphine

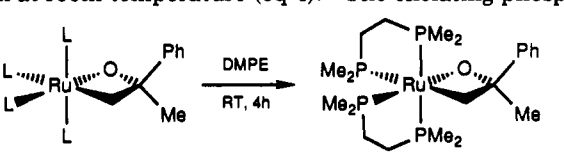

(4)

prevented the problem of phosphine dissociation experienced when attempting to isolate metallacycle **11a**. Therefore, it was possible to obtain pure samples of **11b**, and this complex was characterized by solution NMR spectroscopy, solid-state infrared spectroscopy, and microanalysis. The material was obtained as a white, air-sensitive solid, which was crystalline but tended to form thin plates, precluding an X-ray diffraction study. The compound was stored indefinitely at room temperature in the drybox without decomposition. The ^1H and $^{13}C\{^1H\}$ NMR spectra of **11b** showed eight DMPE methyl groups, and the $^{31}P\{^1H\}$ NMR spectrum displayed an ABCD pattern. The connectivity of the metallacycle portion of the molecule was clear from ^1H NMR and $^{13}C\{^1H\}$ NMR spectroscopy, with $^{13}C\{^1H\}$ NMR assignments based on

Table VI. ^{1}H NMR Spectroscopic Data[a]

compd	δ, ppm	mult[a]	*J*, Hz	int	assignment[b]
cis-$(PMe_3)Ru(Ph)(Cl)$[c,d] (*cis*-**1**)	1.13	d	7.0	9	*cis*-PMe_3
	1.14	t	3.0	18	*trans*-PMe_3
	1.25	d	5.6	9	*cis*-PMe_3
	7.04	m			Ar[j]
	7.58	m			Ar[j]
trans-$(PMe)_4Ru(Ph)(Cl)$[c,d] (*trans*-**1**)	1.33	br s		36	PMe_3
	7.04	m			Ar[j]
	7.58	m			Ar[j]
$(PMe_3)_4Ru(Me)(OC(CMe_2)H)$[d] (**5a**)	0.20	m		3	RuMe
	0.87	d	7.2	9	*cis*-PMe_3
	1.14	t	2.8	18	*trans*-PMe_3
	1.17	d	5.6	9	*cis*-PMe_3
	2.12	s		3	$OC(CMe_aMe_b)H$
	2.15	s		3	$OC(CMe_aMe_b)H$
	6.73	br s		1	$OC(CMe_2)H$
$(PMe_3)_4Ru(Me)(OC(CH_2)H)$[d] (**5b**)	0.16	m		3	RuMe
	0.84	d	7.3	9	*cis*-PMe_3
	1.12	d	5.7	9	*cis*-PMe_3
	1.15	t	2.7	18	*trans*-PMe_3
	3.90	m		1	$OC(CH_aH_b)H$
	4.25	dd	13.2, 2.0	1	$OC(CH_aH_b)H$
	7.25	dd	14.6, 4.8	1	$OC(CH_2)H$
$(PMe_3)_4Ru(Me)(OC(CH_2)CMe_3)$[d] (**5c**)	−0.15	m		3	RuMe
	0.98	s		9	$OC(CH_2)CMe_3$
	1.23	d	7.3	9	*cis*-PMe_3
	1.39	t	2.7	18	*trans*-PMe_3
	1.45	d	5.6	9	*cis*-PMe_3
	3.41	d	1.2	1	$OC(CH_aH_b)CMe_3$
	3.58	br s		1	$OC(CH_aH_b)CMe_3$
$(PMe_3)_4Ru(H)(OC(CH_2)Me)$[d] (**6a**)	−7.74	dq	104, 17.4	1	RuH
	1.01	d	7.3	9	*cis*-PMe_3
	1.13	d	5.5	9	*cis*-PMe_3
	1.37	t	2.9	18	*trans*-PMe_3
	2.07	s		3	$OC(CH_2)Me$
	3.91	d	2.9	1	$OC(CH_aH_b)Me$
	4.16	d	2.9	1	$OC(CH_aH_b)Me$
$(PMe_3)_4Ru(OC(CH_2)C_6H_4)$[g] (**7**)	1.02	t	6	18	*trans*-PMe_3
	1.42	d	6.9	9	*cis*-PMe_3
	1.45	d	6.0	9	*cis*-PMe_3
	3.39	d	1.2	1	$OC(CH_aH_b)C_6H_4$
	3.95	br s		1	$OC(CH_aH_b)C_6H_4$
	6.61	tq	7.3, 1.0	1	$OC(CH_2)C_6H_4$
	6.63	t	7.1	1	$OC(CH_2)C_6H_4$
	7.11	dt	7.6, 1.6	1	$OC(CH_2)C_6H_4$
	7.46	m		1	$OC(CH_2)C_6H_4$
$(PMe_3)_4Ru(Me)(OC(CH_2)Me)$[d] (**8a**)	0.40	m		3	RuMe
	0.86	d	7.4	9	*cis*-PMe_3
	1.18	d	5.3	9	*cis*-PMe_3
	1.27	t	2.8	18	*trans*-PMe_3
	2.06	s		3	$OC(CH_2)Me$
	3.50	d	2.2	1	$OC(CH_aH_b)Me$
	3.96	d	2.2	1	$OC(CH_aH_b)Me$
$(PMe_3)_4Ru(Me)(CH_2(O)Me)$[d] (**8b**)	−0.26	m		3	RuMe
	0.95	d	5.1	9	*cis*-PMe_3
	0.96	d	5.1	9	*cis*-PMe_3
	1.25	t	2.6	18	*trans*-PMe_3
	2.00	s		3	$CH_2C(O)Me$
	not obsd				$CH_2C(O)Me$
$(PMe_3)_4Ru(Me)(OC(CH_2)CH_2CMe_3)$ and $(PMe_3)_4Ru(Me)(CH_2C(O)CH_2CMe_3)$[d,h] (**9a,b**)	−0.33	dtd	8.4, 7.0, 4	3	RuMe
	−0.15	dtd	7.9, 4.0, 3	3	RuMe
	0.88	d	7.3		*cis*-PMe_3[k]
	0.97	d	5.0		*cis*-PMe_3[k]
	0.98	d	5.8		*cis*-PMe_3[k]
	1.29	m			*t*-Bu, *trans*- and *cis*-PMe_3[k]
	1.96	m		2	$CH_2C(O)CH_2CMe_3$
	2.06	s		2	$CH_2C(O)CH_2CMe_3$
	2.15	s		2	$OC(CH_2)CH_2CMe_3$
	3.05	dd	2.1, 1.1	1	$CH_2C(O)CH_aH_bCMe_3$
	3.78	d	2.4	1	$CH_2C(O)CH_aH_bCMe_3$
$(PMe_3)_3Ru(Ph)(O(CCHCMe_2CH_2CMe_2CH_2))$[f] (**10**)	−1.25	s		1	$(O(CCHCMe_2CH_2CMe_2CH_2))$
	0.99	d	7.2	9	*cis*-PMe_3
	1.12	t	3.0	18	*trans*-PMe_3
	1.28	s		2	$(O(CCHCMe_2CH_2CMe_2CH_2))$
	1.46	s		6	$(O(CCHCMe_2CH_2CMe_2CH_2))$
	1.48	s		6	$(O(CCHCMe_2CH_2CMe_2CH_2))$
	1.79	s		2	$(O(CCHCMe_2CH_2CMe_2CH_2))$

Table VI (Continued)

compd	δ, ppm	mult[a]	*J*, Hz	int	assignment[b]
$(PMe_3)_3Ru(Ph)(O(CCHCMe_2CH_2CMe_2CH_2))$[f] (**10**)	6.56	m		3	Ar
	6.76	d	6.6	1	Ar
	7.65	d	7.6	1	Ar
$(PMe_3)_4Ru(OC(Me)(Ph)CH_2)$ (**11e**)[e,j]	1.60	s		3	$(OC(\mathit{Me})(Ph)CH_2)$
	7.06	m		2	$(OC(Me)(\mathit{Ph})CH_2)$
	7.15	dd	6.9, 7.2	1	$(OC(Me)(\mathit{Ph})CH_2)$
	7.30	d	7.2	1	$(OC(Me)(\mathit{Ph})CH_2)$
$(DMPE)_2Ru(OC(Me)(Ph)CH_2)$ (**11b**)[f]	0.29	d	5.8	3	$\mathit{Me}_2PCH_2CH_2P\mathit{Me}_2$
	1.19	d	6.4	3	
	1.26	d	7.9	3	
	1.476	d	5.2	3	
	1.50	d	7.1	3	
	1.59	dd	6.9, 2.1	3	
	1.70	d	6.8	3	
	1.79	dd	6.7, 2.0	3	
	1.22	s		3	$(OC(\mathit{Me})(Ph)CH_2)$
	0.62	m		2	$(OC(Me(Ph)\mathit{CH_2})$
	1.5–2.2	m		8	$Me_2P\mathit{CH_2CH_2}PMe_2$
	7.06	t	7.2	1	$(OC(Me)(\mathit{Ph})CH_2)$
	7.29	m		2	
	7.42	d	7.2	1	
	8.15	d	7.2	1	
$(PMe_3)_4Ru(CH_2C(=CHCMe_3)O)$[d] (**13**)	0.83	d	7.1	9	*cis*-PMe_3
	1.05	d	5.4	9	*cis*-PMe_3
	1.33	t	2.8	18	*trans*-PMe_3
	1.36	m		2	$(\mathit{CH_2}C(=CHCMe_3)O)$
	1.61	s		9	$(CH_2C(=CHC\mathit{Me_3})O)$
	3.75	s		1	$(CH_2C(=C\mathit{HCMe_3})O)$
$(PMe_3)_4Ru((CH_2)_2CO)$[i] (**14**)	1.05	d	5.4	18	*cis*-PMe_3
	1.13	t	2.4	18	*trans*-PMe_3
	1.54	t	7.9	4	$(\mathit{CH_2})_2CO$
$(PMe_3)_4Ru(OCCMe_3CH)$[d] (**16**)	0.97	d	7.3	9	*cis*-PMe_3
	1.12	d	5.5	9	*cis*-PMe_3
	1.38	t	2.7	18	*trans*-PMe_3
	1.40	s		9	$(OCC\mathit{Me_3}CH)$
	5.00	dd	11.2, 4.1	1	$(OCCMe_3\mathit{CH})$
$(PMe_3)_3(CO)Ru(Ph)(Me)$[d] (**17**)	0.33	q	42.4	3	RuMe
	0.89	t	2.7	18	*trans*-PMe_3
	1.02	d	6.2	9	*cis*-PMe_3
	7.13	m		2	Ar
	7.23	m		1	Ar
	7.88	d	6.3	1	Ar
	8.21	br, s		1	Ar
$(PMe_3)_3(CO)Ru(Me)_2$[d] (**20**)	−0.62	dt	9.0, 8.4	3	RuMe
	−0.38	td	7.7, 3.8	3	RuMe
	1.04	d	6.2	9	*cis*-PMe_3
	1.12	t	2.8	18	*trans*-PMe_3

[a] The assignments d and t, when applied to the PMe_3 resonances, are observed patterns, not true multiplicity patterns. Accordingly, the values reported as coupling constants for these resonances are the separations between lines and do not necessarily reflect the true coupling constants. [b] The assignment *trans*-PMe_3 refers to mutually trans PMe_3 ligands. The other phosphines are assigned as *cis*-PMe_3. [c] *cis*- and *trans*-$(PMe_3)_4Ru(Ph)(Cl)$ were obtained as a 1:1.1 ratio of the cis and trans isomers. Overlap of the phenyl resonances of these two isomers prevented integration relative to the PMe_3 resonances. [d] C_6D_6, 20 °C. [e] This complex was generated in solution and used in situ. We were able to assign the methyl and phenyl groups of the metallacycle. The phosphine and methylene resonances could not be unambiguously distinguished from impurity resonances. [f] THF-d_8, −40 °C. [g] THF-d_8, 20 °C. [h] Some of the resonances for the O- and C-bound isomers could not be distinguished because of the nearly 1:1 ratio of isomers. Assignments are indicated when unambiguous. [i] Toluene-d_8, 10 °C. [j] Accurate integrals for the aromatic resonances were prevented by overlap of the signals for *trans*- and *cis*-**1**. [k] Accurate integrals were prevented by overlap of the PMe_3 and *tert*-butyl groups for **9a** and **9b**. [l] The stereochemistry at the metal center is cis unless stated otherwise.

spectra obtained with a DEPT pulse sequence. The methyl group was identified by a singlet resonance at δ 1.22 in the ^1H NMR spectrum and one at δ 41.79 in the $^{13}C\{^1H\}$ NMR spectrum. The appropriate resonances for a static, terminal aryl group were observed in the ^1H and $^{13}C\{^1H\}$ NMR spectrum, and the singlet resonance for the ipso carbon indicated that it was no longer bound to the metal center. Instead, the CH_2 group was bound to ruthenium, as indicated by the multiplet resonance at δ 0.62 in the ^1H NMR spectrum and the doublet of multiplets (J = 44.7 Hz) at δ 1.50 in the $^{13}C\{^1H\}$ NMR spectrum.

The metallacycle portion of **11a** showed features in the ^1H and $^{31}P\{^1H\}$ NMR spectrum similar to those of **11b**. Data for these resonances in **11a** are included in Tables VI–VIII, with the exception of the expected 16-line metal-bound CH_2 resonance, which could not be clearly distinguished from phosphine methyl and impurity resonances in the ^1H NMR spectrum. The phosphine methyl resonances could not be unambiguously distinguished from those of impurities; coupling of these methyl groups to four different phosphorus atoms reduced the peak heights. However, the presence a metal-bound CH_2 group was clear from a $^{13}C\{^1H\}$ NMR spectrum obtained with a DEPT pulse sequence, and the presence of four phosphine ligands was clear from the ABCD pattern in the $^{31}P\{^1H\}$ NMR spectrum. A large trans coupling constant of 363 Hz was obtained from a computer simulation of the spectrum.[18]

(18) Spectral simulations were performed with the standard PANIC program.

Table VII. $^{13}C\{^1H\}$ NMR Spectroscopic Data

compd	δ, ppm	mult[a]	J, Hz	assignment[b]
$(PMe_3)_4Ru(Me)(OC(CMe_2)H)$[c] (**5a**)	−2.75	dq	59.2, 11.5	RuMe
	18.27	td	22.0, 2.9	*trans*-PMe_3
	21.82	d	15.3	*cis*-PMe_3
	23.90	dd	23.7, 1.9	*cis*-PMe_3
	16.47	s		$(OC(CMe_aMe_b)H)$
	21.69	s		$(OC(CMe_aMe_b)H)$
	93.79	d	3.6	$(OC(CMe_2)H)$
	149.94	d	4.3	$(OC(CMe_2)H)$
$(PMe_3)_4Ru(Me)(OC(CH_2)H)$[c] (**5b**)	1.12	dq	58.7, 11.5	RuMe
	18.39	td	12.1, 2.6	*trans*-PMe_3
	21.62	dd	16.4, 2.0	*cis*-PMe_3
	23.77	d	25.1	*cis*-PMe_3
	78.39	d	3.5	$(OC(CH_2)H)$
	162.13	d	4.9	$(OC(CH_2)H)$
$(PMe_3)_4Ru(H)(OC(CH_2)Me)$[c] (**6a**)	20.53	dt	17.5, 2.4	*cis*-PMe_3
	27.27	dm	26.9	*cis*-PMe_3
	22.86	td	12.7, 4.0	*trans*-PMe_3
	25.79	d	4.4	$(OC(CH_2)Me)$
	77.30	s		$(OC(CH_2)Me)$
	168.99	d	4.7	$(OC(CH_2)Me)$
$(PMe_3)_4Ru(OC(CH_2)C_6H_4)$[f] (**7**)	19.40	td	12.6, 2.6	*trans*-PMe_3
	22.28	dt	17.0, 1.7	*cis*-PMe_3
	25.23	dm	23.6	*cis*-PMe_3
	72.90	s		$(OC(CH_2)C_6H_4)$
	120.68	d	1.3	$(OC(CH_2)C_6H_4)$ and Ar
	122.61	d	1.4	
	125.23	m		
	141.27	m		
	152.86	d	3.1	
	176.90	dm	7.7	
	177.71	dq	65.0, 8.2	
$(PMe_3)_4Ru(Me)(OC(CH_2)Me)$[c] (**8a**)	−4.26	dq	60.9, 11.5	RuMe
	19.05	t	8.0	*trans*-PMe_3
	22.74	d	15.8	*cis*-PMe_3
	13.50	d	26.1	*cis*-PMe_3
	27.63	d	3.7	$(OC(CH_2)Me)$
	75.68	s		$(OC(CH_2)Me)$
	169.23	s		$(OC(CH_2)Me)$
$(PMe_3)_4Ru(Me)(CH_2C(O)Me)$[c] (**8b**)	−9.73	dq	56, 12	RuMe
	20.88	t	11.9	*trans*-PMe_3
	23.40	d	18.0	*cis*-PMe_3
	24.17	d	15.4	*cis*-PMe_3
	22.83	m		$(CH_2C(O)Me)$
	33.15	s		$(CH_2C(O)Me)$
	not obs.			$(CH_2C(O)Me)$
$(PMe_3)_4Ru(Me)(OC(CH_2)CH_2CMe_3)$ and $(PMe_3)_4Ru(Me)(CH_2C(O)CH_2CMe_3)$[c,d] (**9a,b**)	19.33	td	12.3, 1.6	*trans*-PMe_3
	20.91	tt	12.1, 2.4	*trans*-PMe_3
	23.33	d	20.7	*cis*-PMe_3
	23.56	d	27.5	*cis*-PMe_3
	24.53	d	16	*cis*-PMe_3
	24.57	d	16	*cis*-PMe_3
	25.23	dm	42.2	$(CH_2C(O)CH_2CMe_3)$
	31.16	s		CH_2CMe_3
	31.29	s		CH_2CMe_3
	31.53	s		CH_2CMe_3
	31.58	s		CH_2CMe_3
	54.27	s		CH_2CMe_3
	58.27	s		CH_2CMe_3
	79.45	s		$(OC(CH_2)CH_2CMe_3)$
	172.07	s		$(OC(CH_2)CH_2CMe_3)$
	218.10	d	6.0	$(CH_2C(O)CH_2CMe_3)$
$(PMe_3)_4Ru(O(CCHCMe_2CH_2CMe_2CH_2))$[e] (**10**)	15.64	t	12.5	*trans*-PMe_3
	22.50	d	23.0	*cis*-PMe_3
	31.27	s		$(O(CCHCMe_2CH_2CMe_2CH_2))$
	32.30	s		$(O(CCHCMe_2CH_2CMe_2CH_2))$
	33.13	s		$(O(CCHCMe_2CH_2CMe_2CH_2))$
	35.13	s		$(O(CCHCMe_2CH_2CMe_2CH_2))$
	47.67	s		$(O(CCHCMe_2CH_2CMe_2CH_2))$
	51.72	s		$(O(CCHCMe_2CH_2CMe_2CH_2))$
	76.97	s		$(O(CCHCMe_2CH_2CMe_2CH_2))$
	119.29	s		Ar
	124.65	s		
	125.97	s		
	133.94	s		
	142.22	d	13.0	
	162.51	m		
	164.98	s		$(O(CCHCMe_2CH_2CMe_2CH_2))$

Table VII (Continued)

compd	δ, ppm	mult[a]	*J*, Hz	assignment[b]
$(PMe_3)_4Ru(OC(Me)(Ph)CH_2)$[d,e] (**11a**)	0.99	dm	49	$(OC(Me)(Ph)CH_2)$
	40.88	s		$(OC(Me)(Ph)(CH_2)$
	93.12	s		$(OC(Me)(Ph)CH_2)$
	123.88	s		Ar
	125.46	s		
	126.55	s		
	126.86	d	19.2	
	129.07	s		
	164.41	s		
$(DMPE)_2Ru(OC(Me)(Ph)CH_2)$ (**11b**)[c]	1.50	dm	44.7	$(OC(Me)(Ph)CH_2)$
	12.32	dd	20.4, 3.9	$Me_2PCH_2CH_2PMe_2$
	13.28	pent	5.9	
	14.02	d	17.6	
	15.99	d	8.1	
	17.38	d	15.5	
	19.97	s		
	20.16	dd	20.9, 4.7	
	23.13	d	16.6	
	29.62	t	21.6	$Me_2PCH_2CH_2PMe_2$
	30.72	dd	28.9, 13.7	
	34.44	dd	26.4, 23.7	
	35.22	dd	31.6, 19.3	
	41.79	s		$(OC(Me)(Ph)CH_2)$
	92.62	s		$(OC(Me)(Ph)CH_2)$
	123.98	s		$(OC(Me)(Ph)CH_2)$
	126.30	s		
	126.84	s		
	126.99	s		
	127.10	s		
	164.21	s		
$(PMe_3)_4Ru(OC(=CHCMe_3)CH_2)$[c] (**13**)	−1.57	dtd	51, 37, 5.1	$(OC(=CHCMe_3)CH_2)$
	18.54	td	12.0, 3.1	*trans*-PMe_3
	22.65	d	16.3	*cis*-PMe_3
	24.85	dd	24.9, 2.2	*cis*-PMe_3
	31.56	s		$(OC(=CHCMe_3)CH_2)$
	32.88	s		$(OC(=CHCMe_3)CH_2)$
	102.64	t	2.8	$(OC(=CHCMe_3)CH_2)$
	179.88	s		$(OC(=CHCMe_3)CH_2)$
$(PMe_3)_4Ru((CH_2)_2CO)$[h] (**14**)	19.06	td	12.4, 1.5	*trans*-PMe_3
	26.23	m		*cis*-PMe_3
	29.13	dq	38. 6	$((CH_2)_2CO)$
	184.00	d	3.0	$((CH_2)_2CO)$
$(PMe_3)_4Ru(OC(CMe_3)CH)$[c] (**16**)	19.27	td	13.1, 2.7	*trans*-PMe_3
	22.93	d	15.7	*cis*-PMe_3
	25.46	dd	25.1, 3.1	*cis*-PMe_3
	29.29	s		$(OC(CMe_3)CH)$
	38.88	s		$(OC(CMe_3)CH)$
	90.86	dtd	64, 16, 6.0	$(OC(CMe_3)CH)$
	174.37	t	5.6	$(OC(CMe_3)CH)$
$(PMe_3)_3(CO)Ru(Me)(Ph)$[e] (**17**)	−6.55	q	11.5	RuMe
	18.27	t	14.0	*trans*-PMe_3
	20.71	d	19.7	*cis*-PMe_3
	121.71	s		Ar
	126.37	d	4.8	
	126.48	s		
	138.59	d	2.1	
	146.83	s		
	166.78	dt	72.7, 17.3	
	200.56	q	10.2	RuCO

[a] The assignments d and t, when applied to the PMe_3 resonances, are observed patterns, not true multiplicity patterns. Accordingly, the values reported as coupling constants for these resonances are the separations between lines and do not necessarily reflect the true coupling constants. [b] The assignment *trans*-PMe_3 refers to mutually trans PMe_3 ligands. The other phosphines are assigned as *cis*-PMe_3. [c] C_6D_6, 20 °C. [d] This complex was generated in solution and used in situ. We were able to assign the resonances of the metallacycle. The phosphine resonances could not be unambiguously distinguished from impurity resonances. [e] THF-d_8, −40 °C. [f] THF-d_8, 20 °C. [g] Some of the resonances for the O- and C-bound isomers could not be distinguished because of the nearly 1:1 ratio of isomers. Assignments are indicated when unambiguous. [h] Toluene-d_8, 10 °C.

The inequivalence of the two trans phosphines is consistent with the phenyl and methyl group bound to the β-position, one on each side of the metallacycle.

A likely intermediate in the conversion of **1** to oxametallacycle **11** is the product of simple substitution **4a**, and we were able to directly observe **4a** spectroscopically. Compound **4a** was generated by addition of the potassium enolate of acetone to the phenyl chloride complex in THF-d_8 solvent at room temperature for <1 min. ^1H NMR spectroscopic analysis at −40 °C displayed olefinic resonances characteristic of an O-bound enolate, as well as a static, terminal aryl group. The $^{31}P\{^1H\}$ NMR spectrum displayed an A_2BC pattern with chemical shifts similar to those of the other enolate complexes described in the synthesis section. Allowing this solution to warm to 20 °C resulted in the conversion of **4a** to **11a** in a yield similar

Table VIII. $^{31}P\{^1H\}$ NMR Spectroscopic Data

compd	spin syst	δ, ppm	J, Hz
cis-$(PMe_3)_4Ru(Ph)(Cl)$ (*cis*-**1**)[a]	A_2BC	δA = −8.08	J_{AB} = 33
		δB = 12.02	J_{AC} = 22
		δC = −15.60	J_{BC} = 25
trans-$(PMe_3)_4Ru(Ph)(Cl)$ (*trans*-**1**)[a]	A_4	−7.94	
$(PMe_3)_4Ru(Me)(OC(CMe_2)H)$ (**5a**)[a]	A_2BC	δA = −0.46	J_{AB} = 32.4
		δB = 14.55	J_{AC} = 26.2
		δC = −11.41	J_{BC} = 16.1
$(PMe_3)_4Ru(Me)(OC(CH_2)H)$ (**5b**)[a]	A_2BC	δA = 0.26	J_{AB} = 33.2
		δB = 15.41	J_{AC} = 26.1
		δC = −12.01	J_{BC} = 16.6
$(PMe_3)_4Ru(Me)(OC(CH_2)CMe_3)$ (**5c**)[d]	A_2BC	δA = −0.83	J_{AB} = 30.6
		δB = 9.37	J_{AC} = 26.0
		δC = −8.91	J_{BC} = 16.5
$(PMe_3)_4Ru(H)(OC(CH_2)Me)$ (**6a**)[a]	A_2BC	δA = 2.12	J_{AB} = 33.0
		δB = 14.18	J_{AC} = 26.7
		δC = −12.63	J_{BC} = 16.4
$(PMe_3)_4Ru(OC(CH_2)(C_6H_4)$ (**7**)[d]	A_2BC	δA = 0.69	J_{AB} = 25.3
		δB = −13.71	J_{AC} = 32.2
		δC = 6.86	J_{BC} = 14.3
$(PMe_3)_4Ru(Me)(OC(CH_2)Me)$ (**8a**)[a]	A_2BC	δA = 0.49	J_{AB} = 34.7
		δB = 16.89	J_{AC} = 24.1
		δC = −13.20	J_{BC} = 16.8
$(PMe_3)_4Ru(Me)(CH_2C(O)Me)$ (**8b**)[a]	A_2BC	δA = −4.88	J_{AB} = 30.1
		δB = −0.73	J_{AC} = 27.5
		δC = −16.93	J_{BC} = 14.7
$(PMe_3)_4Ru(Me)(OC(CH_2)CH_2CMe_3)$ (**9a**)[a]	A_2BC	δA = 0.70	J_{AB} = 36.2
		δB = 16.94	J_{AC} = 21.4
		δC = −14.26	J_{BC} = 19.0
$(PMe_3)_4Ru(Me)(CH_2C(O)CH_2CMe_3)$ (**9b**)[a]	A_2BC	δA = −4.75	J_{AB} = 29.9
		δB = −0.42	J_{AC} = 27.7
		δC = −17.06	J_{BC} = 14.5
$(PMe_3)_3Ru(O(CCHCMe_2CH_2CMe_2CH_2)$ (**10**)[b]	A_2B	δA = 0.82	J_{AB} = 32.6
		δB = 13.54	
$(PMe_3)_4Ru(OC(Me)(Ph)CH_2)$ (**11a**)[b,c]	ABCD	δA = 11.36	J_{AB} = 34.7
		δB = 0.46	J_{AC} = 34.8
		δC = −2.02	J_{AD} = 5.8
		δD = −12.12	J_{BC} = 363.4
			J_{BD} = 26.3
			J_{CD} = 26.5
$(DMPE)_2Ru(OC(Me)(Ph)CH_2)$ (**11b**)[b,c]	ABCD	δA = 67.23	J_{AB} = 28.9
		δB = 56.86	J_{AC} = 10.7
		δC = 53.42	J_{AD} = 17.4
		δD = 47.58	J_{BC} = 9.7
			J_{BD} = 390.2
			J_{CD} = 21.9
$(PMe_3)_4Ru(O(C{=}CHCMe_3)CH_2)$ (**13**)[a]	A_2BC	δA = 1.09	J_{AB} = 32.5
		δB = 11.97	J_{AC} = 23.9
		δC = −12.27	J_{BC} = 8.9
$(PMe_3)_4Ru((CH_2)_2CO)$ (**14**)[e]	A_2B_2	δA = −2.17	J_{AB} = 33.6
		δB = −9.17	
$(PMe_3)_4Ru(OCCMe_3CH)$ (**16**)[a]	A_2BC	δA = −3.43	J_{AB} = 35.0
		δB = 15.58	J_{AC} = 26.2
		δC = −13.28	J_{BC} = 14.47
$(PMe_3)_3(CO)Ru(Me)(Ph)$ (**17**)[a]	A_2B	δA = −4.07	J_{AB} = 24.6
		δB = −13.00	
$(PMe_3)_3(CO)Ru(Me)_2$ (**20**)[a]	A_2B	δA = −0.25	J_{AB} = 24.0
		δB = −12.56	

[a] C_6D_6, 20 °C. [b] THF-d_8, −40 °C. [c] Chemical shifts and coupling constants were obtained from a simulated spectrum. [d] THF-d_8, 20 °C. [e] Toluene-d_8, 10 °C.

to those resulting from simple room temperature addition of the potassium enolate of acetone to **1** in arene solvents.

A study was performed to determine the role phosphine dissociation plays during this rearrangement. A solution of the phenyl enolate complex **4a** was generated by the above procedure and was divided into two NMR tubes. The samples were frozen in liquid nitrogen and to one of them was added 5 equiv of trimethylphosphine (0.12 M). The rate of formation of metallacycle **11a** was measured at 20 °C for the sample containing no added phosphine, by monitoring the disappearance of starting material resonances in the ^1H NMR spectrum. A linear first-order plot for this reaction was obtained over greater than three

Scheme IV

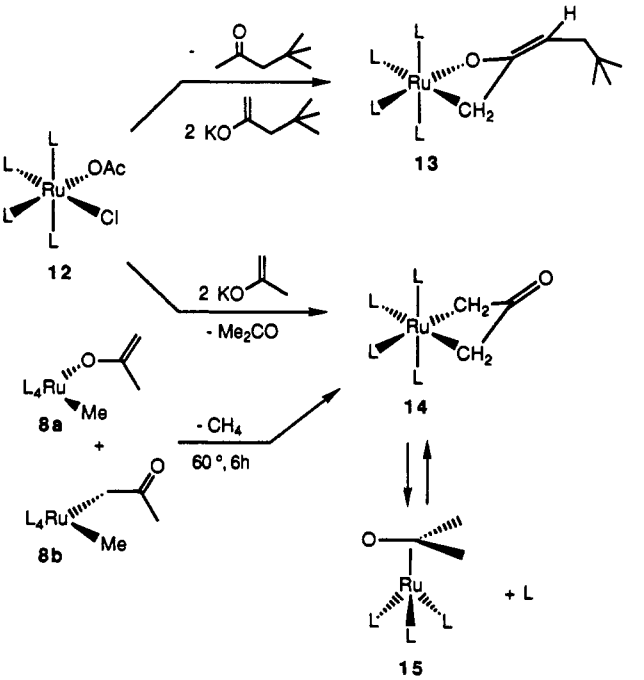

half-lives and provided a rate constant of 4.55×10^{-4} s^{-1}. Thus, the half-life of this reaction was on the order of 25 min. In contrast, the half-life of the sample containing 4 equiv of added phosphine was on the order of 9 h, though a precise rate constant was not obtained for this sample. The rate of this phenyl migration step is, therefore, strongly dependent on the concentration of free PMe_3.

The room temperature addition of 2 equiv of the potassium enolate of 4,4-dimethyl-2-pentanone to $(PMe_3)_4Ru(OAc)(Cl)$ (**12**)[13] led to formation of the oxametallacyclobutane $(PMe_3)_4Ru(OC(=CHCMe_3)CH_2)$ (**13**) in 34% isolated yield, as shown in Scheme IV. This compound was characterized by microanalysis, solution NMR, and solid-state infrared spectroscopy. The ^1H NMR spectrum displayed a multiplet CH_2 resonance at δ 1.36 and a vinylic CH resonance at δ 3.75. Similarly the $^{13}C\{^1H\}$ NMR spectrum contained a doublet of triplet of doublets CH_2 resonance at δ −1.57 and a vinylic CH resonance at δ 102.64. The $^{31}P\{^1H\}$ NMR spectrum consisted of an A_2BC pattern with one phosphine resonating upfield and one downfield of the mutually trans phosphines, consistent with one Ru–O and one Ru–C linkage. Results from an X-ray diffraction study on this compound are reported in a companion paper, which covers structure and reactivity of the ruthenacycles.[8]

Addition of 2 equiv of the potassium enolate of acetone to $(PMe_3)_4Ru(OAc)(Cl)$ (**12**) led to formation of $(PMe_3)_4Ru(\eta^2\text{-}CH_2)_2CO)$ (**14**) and $(PMe_3)_3Ru(\eta^4\text{-}(CH_2)_2CO)$ (**15**) in roughly equal quantities and in 45–55% total yield by ^1H NMR spectroscopy (Scheme IV).[7b] The η^4 complex **15** was isolated in 45–50% yield by sublimation, but we were not able to obtain synthetically useful quantities of **14** due to rapid phosphine dissociation. These two compounds were formed in similar yields by warming a benzene solution of the equilibrium mixture of O- and C-bound enolates **8a** and **8b** to 65 °C for 6 h. The methane byproduct was formed in 95% yield as determined by Toepler pump techniques. Clean samples of metallacycle **14** were generated in solution for NMR spectroscopic characterization by the addition of excess PMe_3 to a solution containing purified tris(phosphine) complex **15**. At 10 °C in toluene solution, compound **14** displayed an A_2B_2

$^{31}P\{^1H\}$ NMR spectrum. The ^1H NMR spectrum is simple and contains only one pseudotriplet CH_2 resonance in addition to the two phosphine methyl resonances. The symmetry required for these two spectra indicates that the ring is planar or is inverting rapidly on the NMR time scale at this temperature. The $^{13}C\{^1H\}$ NMR spectrum contained a doublet of quartets for the metal-bound CH_2 and a doublet for the uncoordinated carbonyl group. This structural assignment was confirmed by an X-ray diffraction study on a single crystal obtained by removing the reaction solvent at low temperature and cooling a pentane solution to −40 °C. A detailed description of the crystal structure of this metallacycle is provided in the following paper.

Warming a solution of $(PMe_3)_4Ru(Me)(OC(CH_2)CMe_3)$ (**5c**) to 65 °C for 8 h led to formation of the oxametallacyclobutene $(PMe_3)_4Ru(OC(CMe_3)CH)$ (**16**) in 39% isolated yield, as displayed in eq 5. Evidence for metalation

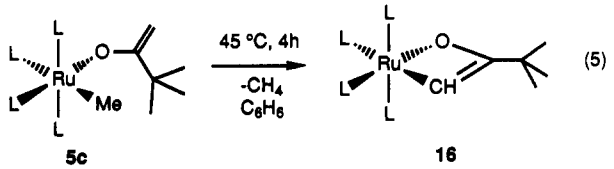

(5)

was obtained from the doublet of triplet of doublets CH resonance in the $^{13}C\{^1H\}$ NMR spectrum (confirmed by DEPT pulse sequence) at δ 90.86, as well as the doublet of doublets CH resonance at δ 5.00. In addition, a methane resonance was observed by ^1H NMR spectroscopy when the thermolysis was performed in a sealed NMR tube. These splitting patterns, resulting from coupling to the phosphine ligands, indicate that the CH group is bound to the metal center. The $^{31}P\{^1H\}$ NMR spectrum displayed an A_2BC pattern with one phosphine resonating upfield and one downfield of the mutually trans phosphine, indicating that one phosphine is located trans to a Ru–O linkage and one trans to a Ru–C linkage.

Reductive Elimination Reactions. Thermolysis of the hydrido enolate complex **6a** led to no reaction up to 85 °C. At 110 °C, decomposition of **6a** occurred to form dihydride $(PMe_3)_4Ru(H)_2$ in low yield, and no formation of acetone was observed. However, addition of 2 atm of CO followed by heating to 85 °C for 8 h led to formation of acetone in 79% yield by ^1H NMR spectroscopy and $(PMe_3)_2Ru(CO)_3$ in 62% yield, as shown in eq 6.

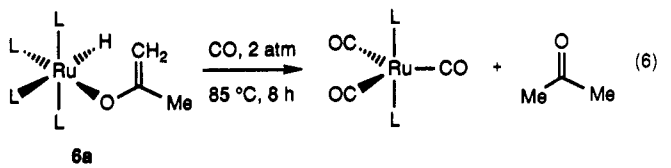

(6)

β-Hydrogen Elimination Reactions. Addition of the potassium enolate of acetaldehyde to the phenyl chloride complex **1** (Scheme V) led to formation of two isomeric complexes **17** and **18**, each containing three phosphines. Warming these two compounds to 45 °C for 4 h led to complete conversion to the major isomer, containing the CO located trans to the ruthenium-bound methyl, $(PMe_3)_3(CO)Ru(Me)(Ph)$ (**17**) in 95% overall yield by ^1H NMR spectroscopy and 23% isolated yield. This compound was characterized by microanalysis, ^1H, $^{13}C\{^1H\}$, and $^{31}P\{^1H\}$ NMR, and infrared spectroscopy. Samples of compound **17** were prepared independently by the addition of 1 equiv of CO to a C_6D_6 solution of $(PMe_3)_4Ru(Me)(Ph)$ at 65 °C, and the ^1H and $^{31}P\{^1H\}$ NMR spectra were identical with those of the isolated material.

Scheme V

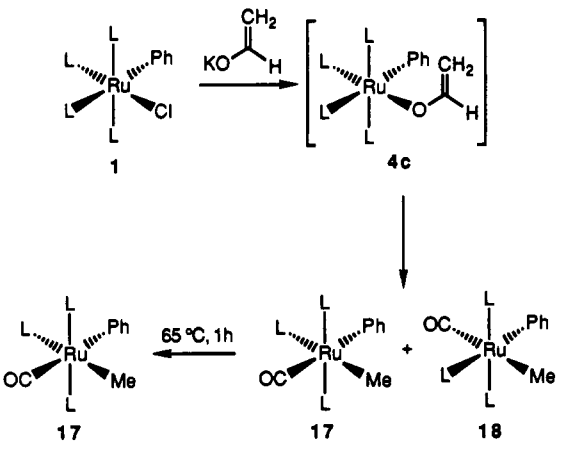

Scheme VI

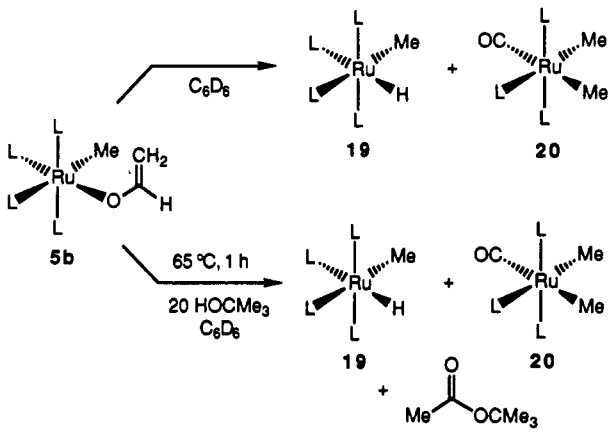

The CO ligand of **17** was identified by a quartet resonance in the $^{13}C\{^1H\}$ NMR spectrum at δ 200.56 and an infrared band at 1898 cm^{-1}. A quartet methyl resonance in the ^1H NMR spectrum at δ 0.33 and a quartet methyl resonance in the $^{13}C\{^1H\}$ NMR spectrum (confirmed by DEPT pulse sequence) at δ −6.55 indicated the presence of a ruthenium-bound methyl group. Resonances for a terminal aryl group were also observed, although all five CH resonances were inequivalent, indicating that rotation of the phenyl group was slow on the ^1H and $^{13}C\{^1H\}$ NMR time scales. The geometry of the molecule was evident from the ipso carbon resonance (a doublet of triplets pattern, with a large J_{PC} of 73 Hz) and the A_2B $^{31}P\{^1H\}$ NMR spectrum. The large coupling in the ipso carbon resonance indicates that it is located trans to a phosphine, and the $^{31}P\{^1H\}$ NMR spectrum indicates the presence of two equivalent phosphines. Thus, the phosphines must be located trans to each other and the CO ligand must be bound trans to the methyl group, consistent with the pseudoquartet splitting pattern for the resonances corresponding to this substituent.

Warming (65 °C, 1 h) a solution of $(PMe_3)_4Ru(Me)(OC(CH_2)H)$ (**5b**), generated from methyl chloride **2** and the potassium enolate of acetaldehyde, led to an 80:14 ratio of methyl hydride $(PMe_3)_4Ru(Me)(H)$ (**19**) and the CO-substituted dimethyl complex $(PMe_3)_3(CO)Ru(Me)_2$ (**20**), as shown in Scheme VI. The total yield of these two compounds was 94% by ^1H NMR spectroscopy. The methyl hydride complex **19** has been previously prepared[9] and was also generated in our laboratory from the addition of C_3H_7MgBr to the methyl chloride complex. The CO-substituted dimethyl complex **20** was identified by ^1H and $^{31}P\{^1H\}$ NMR spectroscopy as well as independent synthesis. Two metal-bound methyl groups were observed at

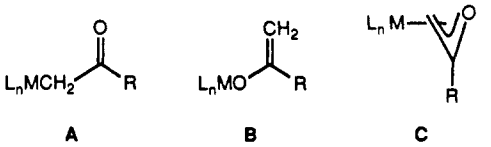

Figure 4. Documented bonding modes for transition-metal enolates.

δ −0.62 and δ −0.38 in the ^{1}H NMR spectrum. An A_2B pattern in the $^{31}P\{^1H\}$ NMR spectrum with chemical shifts similar to those of the CO-substituted phenyl methyl compound **18** indicated the presence of two mutually trans phosphines and one phosphine located trans to a methyl group. This compound was also generated by the addition of 1 equiv of CO to the dimethyl complex $(PMe_3)_4Ru(Me_2)$, followed by heating to 45 °C for 2 days.

The stoichiometry of this reaction raised the possibility that ketene CH_2CO might have been formed as a byproduct of β-hydrogen elimination in **5b**. To test this hypothesis we generated a C_6D_6 solution of the methyl enolate complex **5b**, in the presence of 20 equiv (0.66 M) of *tert*-butyl alcohol as a ketene trap.[19] This hindered alcohol did not react with the starting ruthenium enolate at room temperature and did not significantly affect the total yield or ratio of the two thermolysis products. However, the formation of *tert*-butyl acetate was observed in similar yields (10–15%) in repeated experiments. Increasing the concentration of starting material to 0.1 M and *tert*-butyl alcohol to 2.1 M (20 equiv) with the hope of achieving a higher trapping rate led to low yields of the organometallic product, perhaps due to reaction of the *tert*-butyl alcohol with the starting ruthenium enolate. The reaction was also run in the presence of cyclopentadiene as a ketene trap, but this reagent led to decomposition of methyl enolate **5b** and formation of Cp–ruthenium compounds.

Discussion

Bonding Mode. The usual binding mode for late-transition-metal–enolate complexes is the η^1,C-bound form **A** shown in Figure 4.[5] Recently, an extensive report of the synthesis and catalytic reactivity of rhodium O-bound enolates (**B** in Figure 4) was reported from our laboratory.[3] Two other late-transition-metal O-bound enolates have been reported, although the only spectroscopic data provided for these materials was a ^{1}H NMR spectrum in one case and an infrared spectrum in the other.[4j,k] Examples of isolated η^3-bound enolates are rare,[6] but they have often been invoked as intermediates.[20]

Our results indicate that the free energy difference between the O- and C-bound forms is small for this ruthenium system. The observation of an equilibrium mixture of O- and C-bound enolates and the thermodynamic parameters obtained by variable-temperature NMR spectroscopic studies provided values for ΔH and ΔS that were close to zero. The faster rate of phosphine dissociation, as compared to the rate of interconversion, shows that exchange by way of an η^3-oxallyl intermediate is possible, as shown in Scheme II. If this is the case, the low barrier to interconversion suggests that even the η^3-form is kinetically accessible from both of the η^1-forms and therefore is within 25 or 30 kcal of the ground-state structures.

Scheme VII

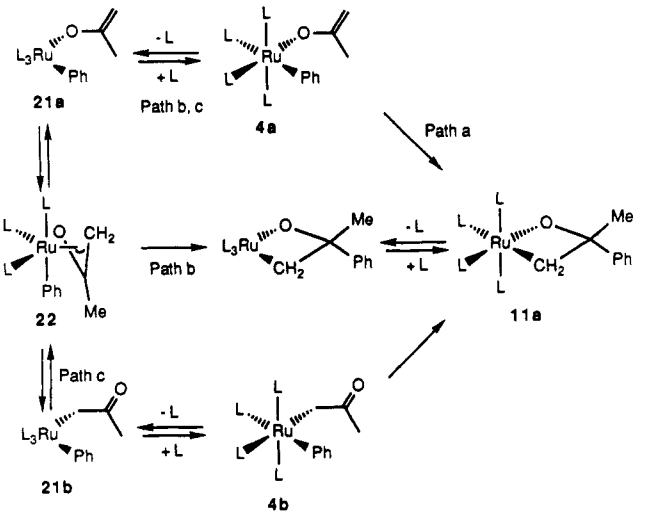

The η^2-binding mode of the enolate of 3,3,5,5-tetramethylcyclohexanone, which incorporates an agostic metal/vinyl hydrogen interaction, reveals a novel form of transition-metal–enolate binding. Once again, a mixture of two forms (η^1 and η^2; 1:1.4) was observed in the crude reaction mixture. The η^2-enolate results from (presumably reversible) dissociation of phosphine from the η^1-complex and indicates that the difference in free energy between the two forms is small. We attribute the unusual η^2-binding mode to the steric bulk of the enolate substituent. We believe that steric interaction with the phosphines causes ligand dissociation but also prevents η^3-coordination, which would bring the methyl groups on the ring prohibitively close to the phosphine methyl groups.

Phenyl Migration. Three possible mechanisms for the formation of oxametallacyclobutane **11a** from phenyl enolate **4a** are shown in Scheme VII. Path a involves migration of the phenyl group directly to the central carbon of the O-bound enolate **4a**. Similarly, path c involves migration within an L_4Ru complex but to the central carbon of the C-bound enolate **4b**. Since the methyl (acetone) enolate complexes **8a** and **8b** rapidly interconvert on the laboratory time scale, the C-bound phenyl (acetone) enolate **4b** may also be present, although its concentration may be too small to detect. Path b proposes that **11a** is formed from **22** in an irreversible step in which the phenyl group migrates to the central carbon of the η^3-bound enolate.

The rate expressions for pathways a and c are both first order in ruthenium complex and do not involve the concentration of free phosphine. Pathway a involves migration of the phenyl group directly to the O-bound isomer **4a** and would display simple first-order kinetic behavior. Reaction by pathway c requires either no phosphine dissociation (if **4a** and **4b** interconvert directly) or both phosphine dissociation and recoordination before the rate-determining step, either of which results in a rate expression that does not involve ligand concentration. The rate of reaction by pathway c would be dependent on phosphine concentration if the formation of **21b** from **22** is irreversible. However, irreversible conversion of **21a** to **21b** seems unlikely since phosphine dissociation with methyl (acetone) enolate compounds **8a** and **8b** occurs faster than interconversion, and equilibration of these two O- and C-bound isomers is complete after 15 min, much faster than the 2 h necessary for conversion of enolate **4a** to metallacycle **11**. We therefore surmise that pathway b involves both dissociation and reassociation of phosphine

(19) March, J. *Advanced Organic Chemistry*; Wiley: New York, 1985; p 685.

(20) (a) Alper, H.; Keung, E. C. H. *J. Org. Chem.* **1972**, *37*, 2566. (b) Prince, R. H.; Raspin, K. A. *J. Chem. Soc. A* **1969**, 612. (c) Goetz, R. W.; Orchin, M. *J. Am. Chem. Soc.* **1963**, *85*, 2782. (d) Shirner, R. L. *Org. React.* **1942**, *1*, 1.

before the rate-determining step, and as a result phosphine terms in the rate expression cancel each other out. However, pathway b involves only dissociation of phosphine before the rate-determining step, and the rate expression for this pathway includes an inverse dependence of rate on phosphine concentration.

Our observation of a marked inverse dependence of rate on phosphine concentration is inconsistent with pathways a and c, in which the rate-determining step involves complexes containing four phosphines. Instead, our results are consistent with a rate-determining step that involves a species resulting from phosphine dissociation. It is possible that phenyl migration occurs in coordinately unsaturated intermediates **21a** or **21b** containing η^1-bound enolates, but we favor migration to the η^3-enolate of intermediate **22** for two reasons. First, it seems unlikely that migration to an η^1-enolate would require predissociation of phosphine. Second, the overall transformation of **4a** to **11a** can be viewed as an insertion of a tethered olefin into the ruthenium–phenyl bond, and many previous studies have demonstrated that olefin insertions into late-metal–alkyl bonds typically proceed by coordination of the olefin followed by migration of the alkyl group.[21] Coordination of the olefin of the enolate in intermediate **21a** before insertion forms oxaallyl **22**.

Metalation Reactions. When the group located cis to the enolate is a methyl group rather than a phenyl ring, a variety of cyclometalation reactions occur to produce oxametallacycles and methane. Metalation of aryl groups is a common process,[22] and metalation of alkyl groups by γ-elimination has been observed with this system and several related ones.[23] Studies with this[10] and other late-metal systems[23b] are consistent with cyclometalation reactions that proceed by way of phosphine dissociation, followed by intramolecular C–H oxidative addition.

Therefore, the type of metallacycle formed by cyclometalation of these ruthenium enolates reflects the selectivity observed in other C–H oxidative addition processes. Formation of metallacycle **14** from the equilibrium mixture of **8a** and **8b** (Scheme IV) shows that either the allylic C–H bond of the O-bound enolate **8a** or the C–H bond α to the carbonyl in the C-bound form **8b** is favored over addition of the vinylic C–H bond of **8a**. Similarly, the formation of **7** (Scheme I) from the methyl enolate intermediate $(PMe_3)_4Ru(Me)(OC(CH_2)Ph)$ (**5d**) demonstrates that addition of the aryl C–H bond to form a five-membered ring is favored over addition of the vinylic C–H bond to form a four-membered ring. In contrast to these results, the vinylic C–H bond in complex **5c** reacts preferentially over the sp^3 C–H bond of the *tert*-butyl group (eq 4). This selectivity forms a four-membered ring over the five-membered ring, which would result from addition of the sp^3 C–H bond, and it parallels previous results,[24] which have demonstrated the greater reactivity of vinylic C–H bonds over alkyl C–H bonds in oxidative addition reactions.

Reductive Elimination Reactions. C–H reductive eliminations are common in alkyl hydride complexes,[25] including an octahedral d^6 rhodium complex containing a C-bound enolate and a hydride ligand.[26] Moreover, we have previously shown that reductive elimination of toluene from the benzyl hydride complex $(PMe_3)_4Ru(H)(CH_2Ph)$ occurs cleanly at 85 °C.[15] Therefore, it is interesting to note that C–H reductive elimination from **6a** preceded by conversion of the O-bound enolate to its C-bound form does not occur at temperatures lower than those that lead to other decomposition pathways.

Direct observation of H–X reductive eliminations (X = N, O) are rare,[27] but when observed they have occurred upon addition of an external ligand. CO-induced H–X reductive elimination reactions, similar to that observed with the O-bound enolate **6a**, have been observed to occur from L_4Ru(hydrido)(aryloxide) and -(arylamide) complexes.[13] However, in none of these cases does irreversible elimination occur directly from the tetrakis(phosphine) complex. Reductive elimination reactions are often favored when electron density at the metal center is reduced, and so perhaps this is why elimination of acetone from **6a** occurs only after initial substitution of the poor σ-donating and strong π-accepting CO for a phosphine ligand.

Scheme VIII

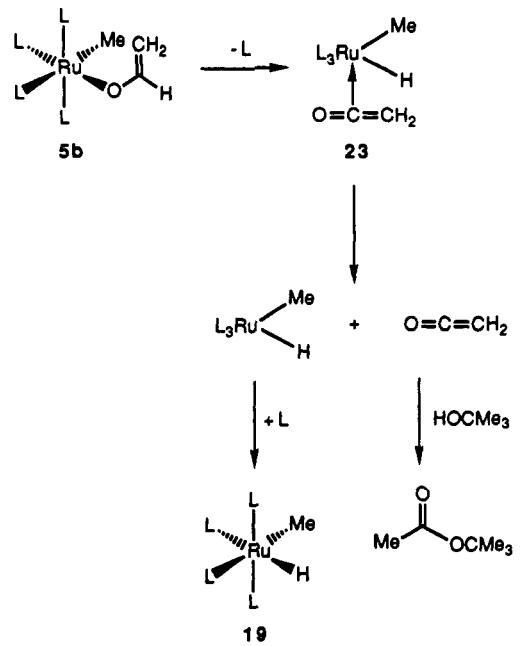

β-Hydrogen Elimination. Our results with the aldehyde enolates provide evidence that β-hydrogen elimination processes occur with these enolate compounds, in contrast to the aldehyde enolates of titanium.[4d] Warming a solution of the methyl enolate **5b** yielded predominantly methyl hydride **19** (Scheme VI). Simple β-hydrogen elimination would form the intermediate **23** with a coordinated ketene, and dissociation of ketene followed by recoordination of phosphine would form the final product **19**, as shown in Scheme VIII. Although we have not obtained extensive evidence for the formation of free ketene during these reactions, our observation of the trapping product *tert*-butyl acetate in 10–15% yield when running the thermolysis of **5b** in the presence of *tert*-butyl

(21) (a) Thorn, D. L.; Hoffmann, R. *J. Am. Chem. Soc.* **1978**, *100*, 2079. (b) Norton, J. R.; Samsel, E. G. *J. Am. Chem. Soc.* **1984**, *106*, 5505. (c) Flood, T. C.; Bitler, S. P. *J. Am. Chem. Soc.* **1984**, *106*, 6076.

(22) Ryabov, A. D. *Chem. Rev.* **1990**, *90*, 403.

(23) See, for example: (a) Andersen, R. A.; Jones, R. A.; Wilkinson, G. *J. Chem. Soc.* **1978**, 446. (b) Foley, P.; DiCosimo, R.; Whitesides, G. M. *J. Am. Chem. Soc.* **1980**, *102*, 6713.

(24) Faller, J. W.; Smart, C. J. *Organometallics* **1989**, *8*, 602.

(25) Collman, J. P.; Hegedus, L. S.; Norton, J. R.; Finke, R. G. *Principles and Applications of Organotransition Meal Chemistry*; University Science Books: Mill Valley, CA, 1987; p 322.

(26) Milstein, D. *Acc. Chem. Res.* **1984**, *17*, 221.

(27) (a) Newman, L. J.; Bergman, R. G. *J. Am. Chem. Soc.*, **1985**, *107*, 5314. (b) Glueck, D. S.; Newman Winslow, L. J.; Bergman, R. G. *Organometallics* **1991**, *10*, 1462. (c) Yamamoto, T.; Sano, K.; Yamamoto, A. *Chem. Lett.* **1982**, 907. (d) Brugo, C. D.; Pasquali, M.; Leoni, P.; Subatino, P.; Braga, D. *Inorg. Chem.* **1909**, *28*, 1390. (e) Cowan, R. L.; Trogler, W. C. *J. Am. Chem. Soc.* **1989**, *111*, 475.

(28) Hartwig, J. F.; Andersen, R. A.; Bergman, R. G. *Organometallics* **1991**, *10*, 1875.

Scheme IX

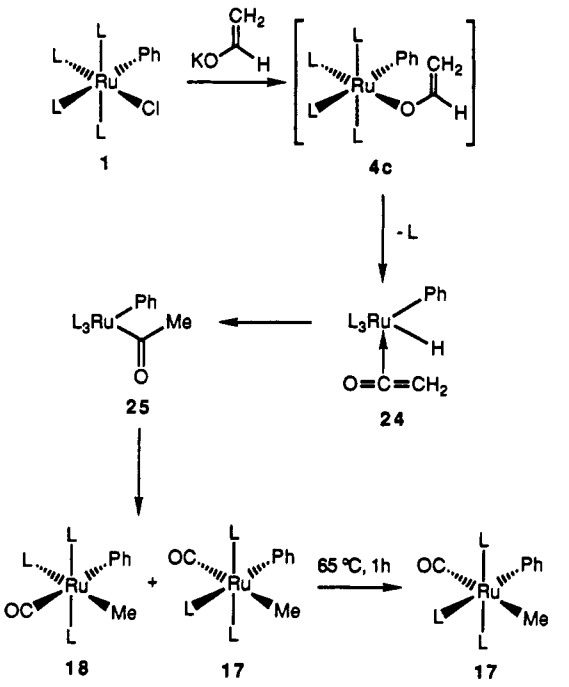

alcohol provide some evidence that either free or coordinated ketene is formed during the course of the reaction.

The CO-substituted dimethyl complex **20** was formed in lower yields by this thermolysis than was methyl hydride complex **19**. However, the analogous CO-substituted methyl phenyl complex **17** was formed in nearly quantitative yield from the addition of the potassium enolate of acetaldehyde to phenyl chloride **1**. A similar cleavage of the enolate of acetaldehyde was observed with cobalt to form a CO and methylene bridged dimer.[29] A probable mechanism for formation of **17** is shown in Scheme IX, and we attribute the formation of **20** to an analogous pathway. Although the phenyl enolate complex **4c** was not observed, the generality of the enolate substitution reactions provides convincing evidence that this compound is the initial intermediate. As proposed for methyl enolate **5b**, we suggest that β-hydrogen elimination forms phenyl hydride **24**, containing a coordinated ketene. Insertion of the ketene C=C bond into the metal hydride bond forms acyl complex **25**, and deinsertion of the acyl carbonyl forms compounds **17** and **18**. We cannot, of course, rule out the possibility that isomerization of **4c** to its C-bound isomer precedes formation of ketene complex **24**.

β-Hydrogen elimination reactions from alkyl[30] and alkoxide[1] complexes are common reaction pathways, but elimination of an sp^2-hybridized β-hydrogen is rare. Relevant examples include the deinsertion of CO_2 from formate complexes.[31] Mechanistic studies of this β-elimination from alkyl groups has demonstrated the importance of an open coordination site on the metal.[30] In addition, the mechanistic information available on the formation of hydrides from formate complexes has pointed to a mechanism that involves coordination of the deinserted CO_2 to an open coordination site.[31] Therefore, we propose mechanisms for the enolate β-hydrogen elimination reactions that involve a coordinated ketene that results from initial phosphine dissociation.

Experimental Section

General. Unless otherwise noted, all manipulations were carried out under an inert atmosphere in a Vacuum Atmospheres 553-2 drybox with an attached M6-40-1H Dritrain or by using standard Schlenk or vaccum line techniques.

^1H NMR spectra were obtained on either the 250-, 300-, 400-, or 500-MHz Fourier transform spectrometers at the University of California, Berkeley (UCB) NMR facility. The 250- and 300-MHz instruments were constructed by Mr. Rudi Nunlist and interfaced with either a Nicolet 1180 or 1280 computer. The 400- and 500-MHz instruments were commercial Bruker AM series spectrometers. ^1H NMR spectra were recorded relative to residual protiated solvent. $^{13}C\{^1H\}$ NMR spectra were obtained at either 75.4, 100.6, or 125.7 MHz on the 300-, 400-, or 500-MHz instruments, respectively, and chemical shifts were recorded relative to the solvent resonance. $^{31}P\{^1H\}$ NMR spectra were obtained at either 120.8 or 161.9 MHz on the 300 or 400 instruments. ^1H and $^{13}C\{^1H\}$ NMR chemical shifts are reported in units of parts per million downfield from tetramethylsilane and $^{31}P\{^1H\}$ NMR chemical shifts are reported in units of parts per million downfield from 87% H_3PO_4. All coupling constants are reported in hertz.

IR spectra were obtained on a Perkin-Elmer Model 283 infrared spectrometer or on a Perkin-Elmer Model 1550 or 1750 FT-IR spectrometer using potassium bromide ground pellets. Mass spectroscopic (MS) analyses were obtained at the UCB mass spectrometry facility on AEI MS-12 and Kratos MS-50 mass spectrometers. Elemental analyses were obtained from the UCB Microanalytical Laboratory.

Sealed NMR tubes were prepared by fusing Wilmad 505-PP and 504-PP tubes to ground glass joints, which were then attached to a vacuum line with Kontes stopcocks. Alternatively, the tubes were attached via Cajon adapters directly to Kontes vacuum stopcocks.[32] Known volume bulb vacuum transfers were accomplished with an MKS Baratron attached to a high vacuum line.

Unless otherwise specified, all reagents were purchased from commercial suppliers and used without further purification. PMe_3 (Strem) was dried over NaK or a Na mirror and vacuum transferred prior to use. Bis(dimethylphosphino)ethane (DMPE) was purchased from Strem and used as received. Mesitylene was dried over sodium/benzophenone ketyl and distilled prior to use. Acetophenone was dried by refluxing over CaH_2, followed by distillation under nitrogen. Hydrogen was purchased from Air Products and was used as received. Acetone was dried with magnesium sulfate before refluxing over magnesium and isolating by vacuum distillation. Carbon monoxide and carbon dioxide were purchased from Matheson and used as received. Trimethylsilane was purchased froom Petrarch and used as received. 4,4-Dimethyl-2-pentanone and pinacolone were purchased from Aldrich and used as received. *tert*-Butylacetylacetone was prepared by the addition of the potassium enolate of 4,4-dimethyl-2-pentanone to *tert*-butylacetyl chloride. *cis*-$(PMe_3)_4Ru(Me)(Cl)$,[8] *cis*-$(PMe_3)_4Ru(OAc)(Cl)$,[13] and $(PMe_3)_4Ru(\eta^2\text{-}C_6H_4)$[10] were prepared according to methods reported previously.

Many of the satisfactory microanalyses were obtained from samples that were pure by NMR but recrystallized before submission. Due to the high solubility of these L_4Ru complexes and the small amounts of material used, yields of recrystallized material were not informative. Yields are reported for once-crystallized samples that were pure by NMR spectroscopy.

Potassium enolates of ketones were formed[33] by the addition of a pentane solution of the ketone to a stirred homogeneous

(29) Halbert, T. R.; Leonowicz, M. E.; Maydonovitch *J. Am. Chem. Soc.* **1980**, *102*, 5107.

(30) Cross, R. J. In *The Chemistry of the Metal-Carbon Bond*; Hartley, R. F., Patai, S., Eds.; Wiley: New York, 1985; Vol. 2., Chapter 8.

(31) See, for example: (a) Darensbourg, D. J.; Wiegreffe, P.; Riordan, C. G. *J. Am. Chem. Soc.* **1990**, *112*, 5759. (b) Darensbourg, D. J.; Fischer, M. B.; Schmidt, R. E., Jr.; Baldwin, B. *J. Am. Chem. Soc.*, **1981**, *103*, 1297. (c) Merrifield, J. H.; Gladysz, J. A. *Organometallics* **1983**, *2*, 782.

(32) Bergman, R. G.; Buchanan, J. M.; McGhee, W. D.; Periana, R. A.; Seidler, P. F.; Trost, M. K.; Wenzel, T. T. In *Experimental Organometallic Chemistry: A Practicum in Synthesis and Characterization*; Wayda, A. L., Darensbourg, M. Y., Eds.; ACS Symposium Series 357; American Chemical Society: Washington, DC, 1987; p 227.

(33) Slough, G. A.; Bergman, R. G.; Heathcock, C. H. *J. Am. Chem. Soc.* **1989**, *111*, 938.

solution of $KN(SiMe_3)_2$ in toluene/pentane 1:100. The precipitated enolate was isolated by filtration and stored in the drybox at −40 °C for up to 1 week. These materials were quite reactive and normally used immediately without further purification or characterization, but NMR analysis typically indicated that they were >85% pure. The potassium enolate of 2-methylpropanal was prepared by the addition of KCH_2Ph[34] to $Me_2SiOCH(=CMe_2)$, which was prepared by standard methods.[35] The potassium enolate of acetaldehyde was formed by allowing a solution of KO-*tert*-Bu and *n*-BuLi in dry tetrahydrofuran to warm to room temperature.[36] The lithium-containing products were removed by washing with toluene and the potassium enolate was isolated by filtration and stored in the drybox at −40 °C for up to several weeks.

Pentane and hexane (UV grade, alkene free) were distilled from $LiAlH_4$ under nitrogen. Benzene, toluene, and tetrahydrofuran were distilled from sodium benzophenone ketyl under nitrogen. Dichloromethane was either distilled under N_2 or vacuum transferred from CaH_2. Deuterated solvents for use in NMR experiments were dried as their protiated analogues but were vacuum transferred from the drying agent.

***cis*- and *trans*-$(PMe_3)_4Ru(Ph)(Cl)$ (1).** To a solution of 100 mg (0.208 mmol) of $(PMe_3)_4Ru(\eta^2\text{-}C_6H_4)$ in 2 mL of ether was added 19.9 mg (1.00 equiv) of Me_3NHCl as a solid. The slurry was stirred for 8 h over which time a yellow solid formed. After this time the solid product (pure 1 by ^1H NMR spectroscopy) was filtered, and the resulting clear solution was cooled to −40 °C to provide yellow blocks of analytically pure product. The solids were combined to yield 63.4 mg (59%) of total product, which was a mixture of the cis and trans isomers. Anal. Calcd for $C_{18}H_{42}ClP_4Ru$: C, 41.74; H, 7.95. Found: C, 41.46; H, 7.95.

***cis*-$(PMe_3)_4Ru(Me)(OC(CMe_2)H)$ (5a).** To a solution of 152 mg (0.334 mmol) of $(PMe_3)_4Ru(Me)(Cl)$ in 4 mL of benzene was added 48 mg (1.3 equiv) of $KOC(CMe_2)H$ as a solid. The slurry was stirred for 4 h at room temperature and then filtered through a medium fritted glass filter, using Celite filter aid. The solvent was removed from the clear yellow filtrate under reduced pressure, and the resulting solid was extracted three times with a total of 10 mL of pentane. The solution volume was reduced to 3 mL in vacuo and cooled to −40 °C to provide 72.4 mg (44%) of analytically pure product. IR (KBr) 1620 (m). Anal. Calcd for $C_{17}H_{46}OP_4Ru$: C, 41.54; H, 9.43. Found: C, 41.61; H, 9.23.

Generation and Spectroscopic Characterization of $(PMe_3)_4Ru(Me)(OC(CH_2)H)$ (5b). To a solution of 154 mg (0.335 mmol) of $(PMe_3)_4Ru(Me)(Cl)$ in 6 mL of benzene was added 54 mg (1.9 equiv) of $KOC(CMe_2)H$ as a solid. The slurry was stirred for 4 h at room temperature after which time an unlocked $^{31}P\{^1H\}$ NMR of an aliquot showed clean conversion to **5b**. The solution was filtered through a medium fritted glass filter, using Celite filter aid. The solvent was removed from the clear yellow/orange filtrate under reduced pressure, and the resulting orange solid was extracted three times with a total of 10 mL of pentane. The solution volume was reduced to 5 mL in vacuo and cooled to −40 °C to provide 16.4 mg (11%) of powder, which was roughly 95% pure by solution NMR. Attempts to obtain analytically pure material were unsuccessful due to partial conversion of **5b** to methyl hydride **19**.

Generation and Spectroscopic Characterization of $(PMe_3)_4Ru(Me)(OC(CH_2)CMe_3)$ (5c). To a solution of 8.2 mg of $(PMe_3)_4Ru(Me)(Cl)$ in 0.6 mL of THF-d_8 was added 7.5 mg (3.1 equiv) of $KOC(CH_2)CMe_3$ as a solid. The resulting solution was placed in an NMR tube and analyzed by ^1H and $^{31}P\{^1H\}$ NMR spectroscopy. It was not possible to isolate pure samples of **5c** due to formation of significant quantities of **16** after several hours at room temperature. Data on **5c** are provided in Tables VI and VIII.

$(PMe_3)_4Ru(H)(OC(CH_2)Me)$ (6a). Into a 1-L glass reaction vessel fused to a Kontes vacuum adaptor was placed a magnetic stir bar and a solution of 350 mg (0.768 mmol) of $(PMe_3)_4Ru(Me)(Cl)$ in 10 mL of C_6D_6. The solution was frozen by immersing the entire vessel in liquid nitrogen. It was exposed to vacuum and then treated with 400 torr of hydrogen. The vessel was closed and warmed to room temperature to provide ~2 atm of hydrogen. The solution was stirred for 24 h, after which time the reaction vessel was opened under argon. $KOCCH_2Me$ (162 mg, 2.2 equiv) was added, and the slurry was stirred for an additional 6 h. An unlocked $^{31}P\{^1H\}$ NMR spectrum of an aliquot showed clean conversion to **6a**. The solvent was removed under reduced pressure, and the resulting yellow residue was extracted three times with a total of 20 mL of pentane. The volume was reduced to 5–6 mL and cooled to −40 °C to provide 176 mg (49%) of analytically pure product. IR (Nujol) 1850 (Ru—H), 1579 (C=C). Anal. Calcd for $C_{15}H_{42}OP_4Ru$: C, 38.87, H, 9.13. Found: C, 38.55; H, 8.99.

$Ru(PMe_3)_4(\eta^2\text{-}OC(CH_2)C_6H_4)$ (7). Preparative Scale. Into a glass reaction vessel fused to a Kontes vacuum adaptor was weighed 31.6 mg (0.0656 mmol) of $(PMe_3)_4Ru(\eta^2\text{-}C_6H_4)$. Benzene (5 mL) was added, and to the resulting solution was added 7.9 mg (1 equiv) of acetophenone. The vessel was heated to 45 °C for 8 h, after which time the initial clear solution had turned yellow. The solvent was removed in vacuo and the product was crystallized from a pentane/toluene (10:1) solvent mixture to yield 13.6 mg (39.5%) of yellow product. IR (KBr) 3103 (m), 3050 (s), 3043 (s), 3028 (m), 2969 (s), 2903 (s), 1977 (w), 1934 (w), 1624 (w), 1569 (s), 1548 (m), 1431 (s), 1395 (s), 1338 (s), 1316 (s), 1298 (s), 1279 (s), 1262 (s), 1238 (m), 1122 (s), 1021 (m), 990 (s), 938 (s), 854 (s), 841 (s), 784 9s), 736 (s), 712 (s), 700 (s), 662 (s), 647 9(s), 634 (m), 498 (m); MS (FAB), *m/e* 525 (MH^+).

$(PMe_3)_4Ru(Me)(OC(CH_2)Me)$ (8a,b). To a solution of 243 mg (0.533 mmol) of $(PMe_3)_4Ru(Me)(Cl)$ in 4 mL of benzene was added 77 mg (1.5 equiv) of $KOC(CH_2)Me$ as a solid. The slurry was stirred for 4 h at room temperature after which time an unlocked $^{31}P\{^1H\}$ NMR of an aliquot showed clean conversion to **8a,b**. The aliquot was returned to the reaction mixture, and the solution was filtered through a medium fritted glass filter, using Celite filter aid. The solvent was removed from the clear yellow filtrate under reduced pressure, and the resulting solid was extracted three times with a total of 10 mL of pentane. The solution volume was reduced to 3 mL and cooled to −40 °C to provide 94.2 mg (37%) of analytically pure enolate product as a mixture of O- and C-bound forms. IR (C_6H_6) 1611 (m), 1583 (s). Anal. Calcd for $C_{16}H_{44}OP_4Ru$: C, 40.24; H, 9.29. Found: C, 40.50; H, 9.14.

Variable-Temperature NMR Spectroscopy of 8a,b. A solution of 24.6 mg of **8a,b** in 0.6 mL of THF-d_8 was placed into an NMR tube equipped with a Kontes vacuum adaptor. The sample was degassed by three freeze, pump, thaw cycles and sealed. Ratios of the two isomers were determined by integrating the metal-bound methyl groups. To ensure that the equilibrium ratio was measured, spectra were obtained in 3-min. intervals at one temperature until the integrated spectra from one pulse acquisitions gave ratios within 10% of one another for three successive spectra. Equilibrium ratios were obtained over the temperature range 5–60 °C. At 5 °C, equilibrium was established over a 15-min time period, and at 60 °C a nonequilibrium ratio was never observed, indicating that equilibrium was established in less than 1 min. The reversibility of the equilibrium was established by obtaining ratios on the same sample at each temperature twice; a second value was measured after initial values were obtained for each temperature. A plot of ln K versus $1/T$ is provided in Figure 2.

$(PMe_3)_4Ru(Me)(OC(CH_2)CH_2CMe_3)$ (9a,b). To a solution of 150 mg (0.329 mmol) of $(PMe_3)_4Ru(Me)(Cl)$ in 4 mL of benzene was added 59 mg (1.2 equiv) of $KOC(CH_2)CH_2CMe_3$ as a solid. The resulting slurry was stirred for 4 h at room temperature after which time an unlocked $^{31}P\{^1H\}$ NMR of an aliquot showed clean conversion to **9a,b**. The aliquot was returned to the reaction mixture, and the solution was filtered through a medium fritted glass filter, using Celite filter aid. The solvent was removed from the clear yellow filtrate under reduced pressure, and the resulting solid was extracted three times with a total of 10 mL of pentane. The solution volume was reduced to 1.5 mL and cooled to −40 °C to provide 76.2 mg (43%) of analytically pure product as a mixture of O- and C-bound forms. IR (Nujol) 1610 (m), 1581 (s). Anal. Calcd for $C_{20}H_{52}OP_4Ru$: C, 45.02; H, 9.82. Found: C, 44.71; H, 9.97.

$(PMe_3)_4Ru(Ph)(O(CCHC(Me_2)CH_2C(Me_2)CH_2))$ (10). To a solution of 126 mg (0.243 mmol) of $(PMe_3)_4Ru(Ph)(Cl)$ in 5 mL

(34) Schlosser, M. *Angew. Chem., Int. Ed. Engl.* **1964**, *3*, 362.
(35) House, H. O.; Czuba, L. J.; Gall, M.; Olmstead, H. D. *J. Org. Chem.* **1969**, *34*, 2324.
(36) Bates, R. B.; Kroposki, L. M.; Potter, D. E. *J. Org. Chem.* **1972**, *37*, 560.

of C_6H_6 was added 180 mg (2.0 equiv) of K(O(CCHC(Me$_2$)-CH$_2$C(Me$_2$)CH$_2$)) as a solid. The solution was stirred for 6 h at room temperature, and an unlocked $^{31}P\{^1H\}$ NMR spectrum of an aliquot showed clean conversion to a product containing four phosphines with an A_2BC spin system ($\delta A = 5.98$, $\delta B = 5.86$, $\delta C = 14.24$, $J_{AB} = 37$, $J_{AC} = 22$, $J_{BC} = 17$) and **10** in a ratio of 1:1.4. The aliquot was returned to the reaction mixture, the solvent was removed under reduced pressure, and the yellow residue was redissolved in 20 mL of toluene and placed into a 100-mL Schlenk flask. The toluene was removed over a 15-min period under reduced pressure while heating the flask at 65 °C. A $^{31}P\{^1H\}$ NMR spectrum obtained on a small portion (5 mg) of the yellow residue showed complete conversion to the tris(phosphine) complex **10**. The remaining residue was extracted into ether and filtered to provide a clear yellow solution. The solution was reduced to 2–3 mL and cooled to −40 °C to provide 66.2 mg (45%) of analytically pure yellow blocks suitable for X-ray structural analysis. IR (THF) 1601. Anal. Calcd for $C_{25}H_{49}OP_4Ru$: C, 53.65; H, 8.83. Found: C, 53.42; 8.86.

Generation and Spectroscopic Observation of (PMe$_3$)$_4$Ru(OC(CH$_2$)Me)(Ph) (4a). To a small vial containing 10.6 mg (0.110 mmol) of KOC(CH$_2$)Me was added a solution of 32.4 mg (0.0626 mmol) of **1** in 0.6 mL of THF-d_8. The yellow solution of **1** immediately turned orange and was placed into an NMR tube equipped with a Kontes vacuum adaptor. The sample was quickly frozen in liquid nitrogen and sealed under vacuum. The tube was then placed into the NMR spectrometer probe at −40 °C. ^1H, $^{31}P\{^1H\}$, and $^{13}C\{^1H\}$ NMR spectroscopy showed clean conversion to phenyl enolate **4a**, and the data obtained are included in Tables VI–VIII.

Generation and Spectroscopic Observation of (PMe$_3$)$_4$Ru(OC(Me)(Ph)CH$_2$) (11a). To a solution of 24.6 mg (0.0475 mmol) of *cis*- and *trans*-(PMe$_3$)$_4$Ru(Ph)(Cl) in 0.6 mL of THF-d_8 was added an excess (9.4 mg, 0.0979 mmol) of KOC(CH$_2$)Me as a solid at room temperature. The suspension was stirred for 2 h over which time the initial yellow solution turned a darker orange, with a fine precipitate. The reaction was then passed through a small plug of Celite, and the resulting clear orange solution was placed into an NMR tube. The tube was equipped with a Kontes vacuum adaptor and sealed under vacuum. ^1H, $^{31}P\{^1H\}$, and $^{13}C\{^1H\}$ NMR spectra were obtained at −40 °C.

(DMPE)$_2$Ru(OC(Me)(Ph)CH$_2$) (11b). To a solution of 85.0 mg (0.164 mmol) of a mixture of *cis*- and *trans*-(PMe$_3$)$_4$Ru(Ph)(Cl) in 8 mL of C_6H_6 was added an excess (40 mg, 0.417 mmol) of KOC(CH$_2$)Me as a solid at room temperature. The resulting yellow suspension was stirred for 2 h, over which time it turned darker orange and a fine precipitate formed. The reaction mixture was then forced through a fritted glass filter with pressure (not vacuum). To the resulting clear orange filtrate was added dropwise at room temperature 2.5 equiv (61.6 mg) of DMPE in 2 mL of Et$_2$O and the resulting solution cooled to −40 °C to yield 38.6 mg (43.9%) of white solid. This material was recrystallized from ether to provide 15.2 mg (17.3%) of analytically pure white crystals. IR (KBr) 2966 (m), 2904 (m), 1596 (m), 1495 (m), 1421 (m), 1292 (m), 1275 (m), 929 (s). Anal. Calcd for $C_{19}H_{42}OP_4Ru$: C, 47.10; H, 7.91. Found: C, 46.81; H, 8.00.

(PMe$_3$)$_4$Ru(OC(=CHCMe$_3$)CH$_2$) (13). To a solution of (PMe$_3$)$_4$Ru(OAc)(Cl) (465 mg, 0.930 mmol) in 15 mL of THF was added 311 mg (2.2 equiv) of KOC(CH$_2$)CH$_2$CMe$_3$ as a solid. After 10 min the solution turned a darker yellow color and an unlocked $^{31}P\{^1H\}$ NMR spectrum of an aliquot showed clean conversion to **13**. The solvent was removed under reduced pressure and the yellow residue was extracted three times with a total of 10 mL of pentane. The resulting slurry was vacuum filtered, and the filtrate was concentrated to 3–4 mL and cooled to −40 °C to provide 162 mg (34%) of product, which was pure by solution NMR spectroscopy. This material was recrystallized from pentane at −40 °C before submitting for microanalysis. IR (KBr) 1594. Anal. Calcd for $C_{19}H_{48}OP_4Ru$: C, 44.09; H, 9.35. Found: C, 43.79; H, 9.40.

(PMe$_3$)$_3$Ru((CH$_2$)$_2$CO) (15). (a) Thermolysis of (PMe$_3$)$_4$Ru(Me)(OC(CH$_2$)Me). Into a glass reaction vessel fused to a Kontes vacuum adaptor was placed a solution of 94.2 mg of (PMe$_3$)$_4$Ru(Me)(OC(CH$_2$)Me) (**8a,b**) in 4 mL of C_6H_6. The solution was degassed by three freeze, pump, thaw cycles and heated to 65 °C for 24 h. The solvent was then removed under reduced pressure while warming the reaction vessel to 45 °C. The resulting solid was extracted three times with a total of 10 mL of pentane. The yellow solution was then concentrated to ~1 mL and cooled to −40 °C to provide 38.2 mg (42%) of product, which was pure by ^1H NMR spectroscopy. This material was recrystallized from pentane before it was submitted for microanalysis. IR (KBr) 1586; MS (FAB, sulfolane) 387 (MH^+), 330 (M − $(CH_2)_2CO^+$). Anal. Calcd for $C_{12}H_{31}OP_4Ru$: C, 37.40; H, 8.10. Found: C, 37.15; H, 8.13.

Alternatively, **15** was prepared without isolation of the enolate intermediate. A solution of the enolate was generated on a 500-mg scale by addition of excess (1.5–3 equiv) potassium enolate to (PMe$_3$)$_4$Ru(Me)(Cl), using the procedure outlined in synthesis of isolated (PMe$_3$)$_4$Ru(Me)(OC(CH$_2$)Me) (**8a,b**). This solution was then filtered and placed into a glass reaction vessel fused to a Kontes vacuum adaptor and heated to 65 °C for 10 h. The product was isolated in 45–55% yield either by isolation and crystallization from pentane as described earlier or by removal of solvent under vacuum and sublimation at 65 °C.

(b) Addition of KOCH$_2$Me to (PMe$_3$)$_4$Ru(OAc)(Cl). To a solution of 512 mg (0.335 mmol) of (PMe$_3$)$_4$Ru(OAc)(Cl) in 6 mL of toluene was added 216 mg (2.2 equiv) of KOC(CMe$_2$)Me as a solid. The resulting slurry was stirred for 4 h at room temperature. The solution was vacuum filtered through a medium fritted glass filter, using Celite filter aid. The clear yellow/orange filtrate was transferred to a 100-mL Schlenk flask and the solvent was removed under reduced pressure while heating the flask to 65 °C. The resulting solid was transferred to a sublimation apparatus, and the product was isolated by sublimation at 65 °C over the course of 24 h to provide 186 mg (47%) of product, which was ca. 90–100% pure by solution NMR spectroscopy.

(PMe$_3$)$_4$Ru((CH$_2$)$_2$CO) (14). (a) Preparation for X-ray Diffraction. Synthetically useful quantities of this compound were not prepared due to its propensity to dissociate phosphine, but we were fortunate enough to obtain a single crystal suitable for an X-ray diffraction study by the procedure described for the formation of (PMe$_3$)$_3$Ru((CH$_2$)$_2$CO) (**15**), with the following modification of the isolation procedure. The benzene solution obtained from thermolysis of the mixture of **8a** and **8b** was frozen at −40 °C, and the solvent was removed by lyophilization. The solid residue was extracted with 10 mL of pentane and the volume reduced to 2 mL at room temperature. Cooling to −40 °C provided several single crystals, one of which was used for an X-ray diffraction study. IR (KBr) 1544 cm^{-1} (C=O).

(b) Preparation for Solution Spectroscopy. Into an NMR tube was placed 0.6 mL of a toluene-d_8 solution containing 35 mg of crystallized tris(phosphine) complex **15**. The tube was equipped with a Kontes vacuum adaptor and degassed by three freeze, pump, thaw cycles. PMe$_3$ (4.0 equiv) was added to the sample by vacuum transfer, and ^1H, $^{31}P\{^1H\}$, and $^{13}C\{^1H\}$ NMR spectroscopy at 10 °C showed rapid formation of the tetrakis(phosphine) complex **14**.

(PMe$_3$)$_4$Ru(OC(CMe$_3$)CH) (16). To a solution of 150 mg (0.329 mmol) of (PMe$_3$)$_4$Ru(Me)(Cl) in 10 mL of THF was added 68.2 mg (1.5 equiv) of KOC(CH$_2$)CMe$_3$ as a solid. The solution was stirred for 4 h at room temperature. The resulting solution of **5c** was then filtered and placed into a glass reaction vessel fused to a Kontes vacuum adaptor. The vessel was heated at 65 °C for 8 h. The solvent was removed under reduced pressure and the solid was crystallized from pentane at −40 °C to provide 64.3 mg of product, which was pure by solution NMR spectroscopy. This material was recrystallized from pentane for microanalysis. IR (KBr) 1591 (m). Anal. Calcd for $C_{18}H_{46}OP_4Ru$: C, 42.94; H, 9.34. Found: C, 43.25; H, 9.19.

Reductive Elimination of Acetone from (PMe$_3$)$_4$Ru(H)(OC(CH$_2$)Me) (6a). Into an NMR tube was placed 0.6 mL of a C_6D_6 solution containing 6.4 mg of (PMe$_3$)$_4$Ru(H)(OC(CH$_2$)Me) and 2 mg of mesitylene as an internal standard. The tube was equipped with a Kontes vaccum adaptor. The sample was immersed in liquid nitrogen and exposed to vacuum, followed by 450 torr of CO. The tube was sealed at the top of the liquid nitrogen. This procedure provides a sample containing 2 atm of CO at 25 °C. A ^1H NMR spectrum was obtained of this initial mixture. The solution was then heated at 85 °C for 24 h, after which time ^1H NMR spectroscopy showed formation of acetone

(79%) and $(PMe_3)_2Ru(CO)_3$ in 62% yield, as determined by comparison to the initial sample prepared independently in our laboratory during the course of a separate study.[37]

$(PMe_3)_3(CO)Ru(Ph)(Me)$ (17). (a) On a Preparative Scale from $(PMe_3)_4Ru(Ph)(Cl)$ and $KO(CCH_2)H$. To a solution of 156 mg (0.301 mmol) of $(PMe_3)_4Ru(Ph)(Cl)$ in 6 mL of ether was added 55 mg (2.2 equiv) of $KOC(CH_2)H$ as a solid. The solution was stirred at room temperature for 4 h, after which time the solid was removed by filtration. The resulting clear, pale yellow solution was concentrated to 1–2 mL, layered with 10 mL of hexanes, and cooled to −40 °C to provide 30.7 mg (22.7%) of white crystals, judged pure by solution NMR spectroscopy. IR(THF) 1898 cm^{-1}.

(b) From $(PMe_3)_4Ru(Ph)(Cl)$ and $KO(CCH_2)H$ To Determine NMR Yield. $(PMe_3)_4Ru(Ph)(Cl)$, 15.2 mg (0.294 mmol), and 2 mg of mesitylene as an internal standard were dissolved in 1.2 mL of THF-d_8. The solution was divided equally into two NMR tubes. To one sample was added 1.8 mg (1.5 equiv) of $KOC(CH_2)H$. After 2 h at 45 °C, ^1H and $^{31}P\{^1H\}$ NMR of the two samples showed a 95% yield of $(PMe_3)_3(CO)Ru(Ph)(Me)$.

(c) From $(PMe_3)_4Ru(Me)(Ph)$ and CO. Into an NMR tube was placed a solution of 8.2 mg (0.017 mmol) of $(PMe_3)_4Ru(Me)(Ph)$ in 0.6 mL of C_6D_6. The tube was equipped with a Kontes vacuum adaptor, and the sample was degassed by two freeze, pump, thaw cycles. One equivalent of CO was added to the sample, as determined by calculating the volume of the NMR tube and adding the appropriate pressure of CO while the NMR tube was immersed in liquid nitrogen (77 K). The tube was then sealed at the top of the liquid nitrogen. Heating the sample to 65 °C for 24 h provided a sample whose ^1H and $^{31}P\{^1H\}$ NMR spectra matched those for material isolated by procedure a.

Addition of $KOC(CH_2)H$ to $(PMe_3)_4Ru(Me)(Cl)$ (2). Into an NMR tube was placed 0.7 mL of a THF-d_8 solution containing 8.4 mg (0.018 mmol) of $(PMe_3)_4Ru(Me)(Cl)$ and 2 mg of mesitylene as an internal standard. A ^1H NMR spectrum was obtained to use in calculating an NMR yield after addition of the enolate. To this sample was added 4 mg (3 equiv) of $KOC(CH_2)H$ as a solid. The NMR tube was equipped with a Kontes vacuum adaptor and sealed under vacuum. The sample was heated at 65 °C for 1 h, after which time ^1H NMR spectroscopy showed formation of $(PMe_3)_4Ru(Me)(H)$[9] in 80% yield and $(PMe_3)_3(CO)Ru(Me)_2$ in 14% yield. The THF-d_8 solvent was then removed under reduced pressure and replaced with C_6D_6 for identification of the two products by comparison of their ^1H and $^{31}P\{^1H\}$ NMR spectra to those reported in C_6D_6 solvent and those obtained by independent synthesis of $(PMe_3)_3(CO)Ru(Me)_2$. Samples of $(PMe_3)_4Ru(Me)(H)$ were also prepared in our laboratory by the addition of $CH_3CH_2CH_2MgBr$ to a THF solution of $(PMe_3)_4Ru(Me)(Cl)$, and the solution NMR spectroscopic data obtained from this preparation were consistent with literature values and those obtained by the above procedure.

Addition of $KOC(CH_2)H$ to $(PMe_3)_4Ru(Me)(Cl)$ (2) in the Presence of $HOCMe_3$. Into a small vial was placed 0.7 mL of a THF solution containing 9.1 mg (0.020 mmol) of $(PMe_3)_4Ru(Me)(Cl)$. To this sample was added 4.9 mg (3.0 equiv) of $KOC(CH_2)H$ as a solid. The slurry was stirred for 0.5 h after which time the ^1H NMR of this mixture showed formation of $(PMe_3)_4Ru(Me)(OC(CH_2)H)$. The solvent was removed under reduced pressure and the resulting crude ruthenium enolate was dissolved in 0.7 mL of C_6D_6. The solid remaining in this mixture was removed by forcing the solution through a small plug of Celite. The clear yellow/orange filtrate was then placed into an NMR tube and to this sample was added 15 μL (20.0 equiv) of $HOCMe_3$ to provide a 0.66 M solution of the alcohol. The NMR tube was then equipped with a Kontes vacuum adaptor, degassed by three freeze, pump, thaw cycles, and sealed. The resulting sample was then heated to 65 °C for 1 h, and analysis by ^1H NMR spectroscopy showed that the two organometallic products were formed in roughly the same yield as in the absence of the alcohol. ^1H NMR spectroscopy also showed the presence of $Me_3COC(O)Me$ in 10–15% yield, as compared to an 80% yield of $(PMe_3)_4Ru(Me)(H)$. The sample was then opened and the solution was forced through a short column of silica, eluting with 1–2 mL of ether to separate the metal-containing products from the organic materials. Gas chromatographic analysis showed the presence of $Me_3COC(O)Me$, as determined by coinjection with an authentic sample.

Independent Generation of $(PMe_3)_3(CO)Ru(Me)_2$ (20). Into an NMR tube was placed a solution of 7.4 mg (0.017 mmol) of $(PMe_3)_4Ru(Me_2)$ in 0.6 mL of C_6D_6. The tube was equipped with a Kontes vacuum adaptor, and the sample was degassed by two freeze, pump, thaw cycles. One equivalent of CO was added to the sample, as determined by calculating the volume of the NMR tube and adding the appropriate pressure of CO while the tube was immersed in liquid nitrogen (77 K). The tube was then sealed at the top of the liquid nitrogen. Heating to 65 °C for 48 h provided a sample whose ^1H and $^{31}P\{^1H\}$ NMR spectra matched those of material formed by the addition of $KOC(CH_2)H$ to $(PMe_3)_4Ru(Me)(Cl)$.

X-ray Crystal Structure Determination of 7. (a) Isolation and Mounting. Crystals of the compound were obtained by slow crystallization from toluene/pentane (1:100) at −40 °C. Fragments cleaved from some of these crystals were mounted in thin-wall capillaries in the air. The capillaries were then flushed with dry nitrogen and flame-sealed. Preliminary precession photographs indicated triclinic Laue symmetry and yielded approximate cell dimensions.

The crystal used for data collection was then transferred to our Enraf-Nonius CAD-4 diffractometer and centered in the beam. Automatic peak search and indexing procedures yielded a triclinic reduced primitive cell. Inspection of the Niggli values revealed no conventional cell of higher symmetry. The final cell parameters and specific data collection parameters for this data set are given in Table I.

(b) Structure Determination. The 3392 raw intensity data were converted to structure factor amplitudes and their esd's by correction for scan speed, background, and Lorentz and polarization effects. No correction for crystal decomposition was necessary. Inspection of the azimuthal scan data showed a variation $I_{min}/I_{max} = 1\%$ for the average curve. No correction for absorption was applied. The choice of the centric space group was confirmed by the successful solution and refinement of the structure.

The structure was solved by Patterson methods and refined via standard least-squares and Fourier techniques. In a difference Fourier map calculated following the refinement of all non-hydrogen atoms with anisotropic thermal parameters, peaks were found corresponding to the positions of most of the hydrogen atoms. Hydrogen atoms were assigned to idealized locations and values of B_{iso} approximately 1.25 times the B_{eqv} of the atoms to which they were attached. They were included in structure factor calculations, but were not refined. Before the last cycles of refinement, 11 data that showed evidence of interference by multiple diffraction were removed from the data set.

The final residuals for 236 variables refined against the 3174 accepted data for which $F_o > 3\sigma(F^2)$ were $R = 1.80\%$, $R_w = 2.90\%$, and GOF = 2.154. The R value for all 3381 data was 2.22%. In the final cycles of refinement a secondary extinction parameter was included (maximum correction: 9% on F).

The quantity minimized by the least-squares program was $\sum w(|F_o| - |F_c|)^2$, where w is the weight of a given observation. The p-factor, used to reduce the weight of intense reflections, was set to 0.02 in the last cycles of refinement. The analytical forms of the scattering factor tables for the neutral atoms were used and all scattering factors were corrected for both the real and imaginary components of anomalous dispersion.

Inspection of the residuals ordered in ranges of $\sin\theta/\lambda$, $|F_o|$, and parity and values of the individual indexes showed no unusual features or trends. The largest peak in the final difference Fourier map had an electron density of 0.24 $e^-/Å^3$ and the lowest excursion −0.19 $e^-/Å^3$.

The positional and thermal parameters of the non-hydrogen atoms are available as supplementary material.

X-ray Crystal Structure Determination of 10. (a) Isolation and Mounting. Crystals of the compound were obtained by slow evaporation of a pentane solution and were mounted in a viscous oil. X-ray data were collected as for 7; the final cell parameters and specific data collection parameters are given in Table I.

(37) Burn, M. J.; Bergman, R. G.; Andersen, R. A., unpublished results.

(b) Structure Determination. The 3860 raw intensity data were converted to structure factor amplitudes and their esd's by correction for scan speed, background, and Lorentz and polarization effects. An empirical absorption correction based on azimuthal scan data (T_{max} = 1.000, T_{min} = 0.959) was applied. Inspection of the systematic absences indicated space group $P2_1/n$. Removal of systematically absent and redundant data left 3771 unique data in the final data set.

The structure was solved by Patterson methods and refined via standard least-squares and Fourier techniques. The final residuals for 141 variables refined against the 3230 data for which $F_2 > 3\sigma(F^2)$ were R = 5.4%, R_w = 8.4%, and GOF = 3.83. The R value for all 2890 data was 6.3%.

The quantity minimized by the least-squares program was $\sum w(|F_o| - |F_c|)^2$, where w is the weight of a given observation. The p factor, used to reduce the weight of intense reflections, was set to 0.03 throughout the refinement. The analytical forms of the scattering factor tables for the neutral atoms were used and all scattering factors were corrected for both the real and imaginary components of anomalous dispersion.

The positional and thermal parameters of the non-hydrogen atoms are provided as supplementary material, as well as a listing of the values of F_o and F_c.

Acknowledgment. We greatly appreciate support for this work from the National Institutes of Health (Grant GM-25459). Crystal structures were performed by Dr. Frederick J. Hollander at the University of California, Berkeley (CHEXRAY) facility.

Supplementary Material Available: Tables of positional parameters, anisotropic thermal parameters, and anisotropic displacements for compounds 7 and 10, as well as the positions and thermal parameters of hydrogen atoms (6 pages); structure factor tables for 7 and 10 (42 pages). This material is provided with the archival edition of the journal, available in many libraries; alternatively, ordering information is given on any current masthead page.

Structure and Reactions of Oxametallacyclobutanes and Oxametallacyclobutenes of Ruthenium

John F. Hartwig, Robert G. Bergman,* and Richard A. Andersen*

Department of Chemistry, University of California, Berkeley, California 94720

Received March 26, 1991

Structure and reactivity studies are reported with the ruthenium metallacycles prepared as described in the previous paper. A C–C cleavage reaction by an apparent β-Me elimination pathway at 45 °C is reported for the PMe_3-substituted oxametallacyclobutane complex $(PMe_3)_4Ru(OC(Me)(Ph)CH_2)$ (1), while the analogous DMPE-substituted metallacyclobutane $(DMPE)_2Ru(OC(Me)(Ph)CH_2)$ (2) is stable at 140 °C. Similarly, compound 1 undergoes insertion of CO into the metal–carbon bond, while 2 is inert toward this substrate. Addition of protic acids and electrophiles leads to rapid extrusion of α-methylstyrene with both metallacycles. X-ray structural analysis of the acetone dianion complex $(PMe_3)_4Ru((CH_2)_2CO)$ (17) was performed and displays a dihedral angle of 46 °C in the metallacycle. In contrast, the 4,4-dimethyl-2-butanone dianion complex $(PMe_3)_4Ru(CH_2C(CHCMe_3)O)$ (15) contains a flat metallacycle that is bound through the CH_2 group and the oxygen atom. Reactivity studies with 15 showed that, unlike compounds 1 and 2, the organic portion remained intact upon addition of protic acids. The addition of 4,4-dimethyl-2-butanone led to a second C–C cleavage reaction, forming the di-*tert*-butylacetylacetonate complex $(PMe_3)_3Ru(Me)(CH(COCH_2CMe_3)_2)$ (19). Reactivity studies with 17 showed reversible formation of the isolable oxatrimethylenemethane complex 18, which was isolated and structurally characterized. Addition of acetone to 17 led to formation of mesityl oxide dianion complex $(PMe_3)_4Ru(OC(Me)CHC(Me)CH)$ (19); mesityl oxide is presumably formed by aldol condensation at the metal center. Reactivity studies of the oxametallacyclobutene complex $(PMe_3)_4Ru(OC(CMe_3)CH)$ showed formation of free ketone upon addition of protic acids and insertion into the metal–oxygen bond upon addition of CO_2. The metallacycle was converted to the silyl enol ether upon addition of trimethylsilane and to the free ketone following addition of H_2.

Introduction

Oxametallacyclobutanes have been invoked as intermediates in several reactions that have found widespread utility. For example, processes such as carbonyl methylenation reactions mediated by transition-metal complexes and asymmetric epoxidation of allylic alcohols with titanium catalysts are believed to involve oxametallacyclobutane intermediates.[1] In addition, the intermediacy of oxametallacycles in the epoxidation of olefins by cytochrome P-450 catalysts has been a controversial topic,[1] and the ability to prepare such metallacycles may help to understand these oxidation processes more fully. Several other reactions of potential utility, such as rhodium-catalyzed synthesis of β-lactams from aziridines[2] and formation of a metallacyclic carbonate of platinum from epoxide and CO_2,[3] are also believed to proceed by way of oxa- and azametallacyclobutanes.

These results demonstrate that even isolable oxametallacyclobutanes should behave as reactive species. In

(1) For discussions of oxametallacyclobutanes as intermediates in titanium-mediated carbonyl methylenation reactions, see: (a) Brown-Wensley, K. A.; Buchwald, S. L.; Cannizzo, L.; Clawson, L.; Ho, S.; Meinhardt, D.; Stille, J. R.; Straus, D.; Grubbs, R. H. *Pure Appl. Chem.* **1983**, *55*, 1733. As intermediates in asymmetric epoxidations, see: (b) Sharpless, K. B.; Teranishi, A. Y.; Backvall, J.-E. *J. Am. Chem. Soc.* **1977**, *99*, 3120. (c) Rappe, A. K.; Goddard, W. A. *J. Am. Chem. Soc.* **1982**, *104*, 3287. With P-450 models, see: (d) Collman, J. P.; Brauman, J. I.; Meunier, B.; Raybuck, S. A.; Kodadek, T. *Proc. Natl. Acad. Sci. U.S.A.* **1984**, *81*, 3245. (e) Walba, D. M.; DePuy, C. H.; Grabowski, J. J.; Bierbaum, V. M. *Organometallics* **1984**, *3*, 498. (f) Collman, J. P.; Kodadek, T.; Raybuck, S. A.; Brauman, J. I.; Papazian, L. M. *J. Am. Chem. Soc.* **1985**, *107*, 4343. (g) Collman, J. P.; Brauman, J. I.; Meunier, B.; Hayashi, T.; Kodadek, T.; Raybuck, S. A. *J. Am. Chem. Soc.* **1985**, *107*, 2000. (h) Mock, W. L.; Bieniarz, C. *Organometallics* **1985**, *4*, 1917. (i) Groves, J. T.; Avaria-Nesser, G. E.; Fish, K. M.; Imachi, M.; Kuczkowski, R. L. *J. Am. Chem. Soc.* **1986**, *108*, 3837. (j) Girardet, M.; Meunier, B. *Tetrahedron Lett.* **1977**, 2955. (k) For a general review, see: Jorgensen, J. A.; Schiott, B. *Chem. Rev.* **1990**, *90*, 1483.

0276-7333/91/2310-3344$02.50/0